IEEE Access
Multidisciplinary | Rapid Review | Open Access Journal

Received 3 November 2022, accepted 12 November 2022, date of publication 21 November 2022,
date of current version 30 November 2022.

Digital Object Identifier 10.1109/ACCESS.2022.3223714

RESEARCH ARTICLE

Three Dimensional Volume Coverage in Multistatic Sonar Sensor Networks

ALPER AVCIOGLU[1,2], (Graduate Student Member, IEEE), ALPER BEREKETLI[3], (Member, IEEE), AND OMER FARUK BAY[4]

[1]Department of Information Systems, Gazi University, 06680 Ankara, Turkey
[2]Defence Systems Technologies Division, Aselsan Inc., 06200 Ankara, Turkey
[3]Communication and Information Technologies Division, Aselsan Inc., 06200 Ankara, Turkey
[4]Department of Electrical-Electronics Engineering, Gazi University, 06560 Ankara, Turkey

Corresponding author: Alper Avcioglu (aavcioglu@aselsan.com.tr)

ABSTRACT Recent changes in the design of enemy threats such as submarines and the technological achievements in sensor development have paved the way for multistatic sonar applications, which increase security and situational awareness in underwater tactical operations. Previously, coverage in multistatic sonar sensor networks (MSSN) was studied using Cassini ovals and the traditional sonar detection model in two dimensions without any discussion of the practicability and feasibility in terms of conditions related to the underwater acoustic propagation environment. In this study, a practical three-dimensional MSSN channel model is proposed. The proposed model covers a spectral variation of absorption loss, ambient noise, sound speed profile, and shadow zones. The realistic effects of sound propagation and environmental conditions are modeled and evaluated using Lybin, which is a well-known sonar performance prediction tool. Using the practical MSSN channel model, the number of source-receiver pairs required to cover a three-dimensional MSSN volume is calculated. The impacts of frequency, source-to-receiver distance, and source level are investigated. The results are compared to the Cassini oval and traditional sonar detection models via an error expression derived according to our verified practical model. The results reveal that the inclusion of ambient conditions and sound propagation characteristics in the channel model leads to huge error levels of 4700000% in the Cassini oval model and 170000% in the traditional sonar detection model, depending on frequency. Thus, the applicability of these models in realistic MSSN deployment scenarios is limited.

INDEX TERMS Anti-submarine warfare, cassini ovals, channel model, multistatic sonar, multistatic sonar sensor networks, situational awareness, sonar detection, volume coverage.

I. INTRODUCTION

Recent conceptual advancements in anti-submarine warfare (ASW), such as the joint deployment and cooperation of autonomous underwater vehicles and unmanned surface vehicles, and the development of new submarines, have necessitated re-evaluating the concepts of maritime safety and underwater situational awareness [1], [2], [3], [4]. Within this scope, active and passive sonar sensors are used to detect underwater threats.

In sonar operations using passive sensors, the detection performance of the receivers depends on both acoustic environmental noise and acoustic noise emitted from the target [5].

Unlike passive sonar sensors, active sonar sensors consist of source-receiver pairs. The basic working principle of the system is that the acoustic wave transmitted from the source is detected by the receiver following its reflection from the target [6]. In monostatic systems, which are traditional active sonar systems, the source and receiver are located in the same place, as shown in Fig. 1a. Systems consisting of a source and a receiver located in different locations are called bistatic sonar systems, as shown in Fig. 1b.

In the past, passive sensors have been quite effective in finding enemy submarines. However, the new generation of submarines is quieter and has advanced stealth capabilities

The associate editor coordinating the review of this manuscript and approving it for publication was Byung-Seo Kim.

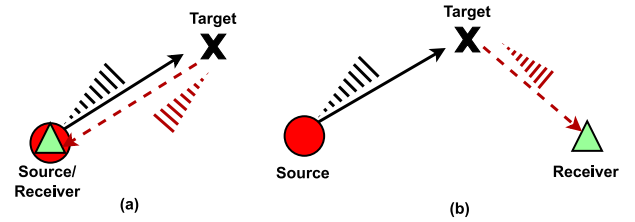

FIGURE 1. (a) A monostatic sensor with a co-located source and receiver, (b) a bistatic system with one source and one independent receiver.

owing to technological advances such as lowering their noise profile, reducing their reflectivity with the use of special rubber tile layers, and lowering the need for snorkeling. Therefore, passive sonar sensors alone are insufficient to detect high-value threat elements such as submarines [7], [8].

At this point, Coon's proposal to combine sources and receivers in surveillance activities is critical, as it enables a more efficient and low-cost deployment solution [9]. Multistatic sonar sensor networks (MSSN) consist of a high-power source and multiple receivers are located at different locations. The receivers detect the acoustic reflections of the source transmission from the target [10].

The MSSN architecture has the following advantages over monostatic sensor deployment [11], [12]:

- Flexibility: Multistatic systems are more flexible in terms of frequency bands and types of platforms. As illustrated in Fig. 2, the system may involve a ship with a towed array or a hull-mounted sonar, a helicopter with dipping sonar, an aircraft-launched sonobuoy, or an unmanned underwater vehicle. Additionally, it is possible to employ various waveforms at various sources, and ping times may be selected with more flexibility in multistatic systems [13], [14].
- Cost-effective coverage: Receivers cost less than sources. With the use of fewer sources and many cheap receivers instead of monostatic sensors, the system's total cost can be reduced without loss of performance.
- Anti-stealth of the platform: While the threat platform can discover active source locations, receivers do not expose their positions due to their passive nature. Since the source and receivers are separated in a multistatic system, concealing the receiver locations makes it more difficult for the hostile target to avoid detection.
- Low false alarm rate: Since multiple sensor receivers can be used, target detection and localization will be more accurate with fewer false alarms. Additionally, with the automatic target recognition feature, operator-related errors in the system detection performance are eliminated [15], [16].

The detection performance of MSSN is directly related to sensor deployment and coverage. In MSSN, deployment can be performed in two ways. Firstly, regarding the location of sensors and communication topologies, a predetermined bottom grid deployment approach can be used for sensor deployment. Secondly, it can be performed in the form of random deployment, where it is not necessary to prearrange the sensor node location and communication topologies for sensor placement [17].

Three different types of coverage problems, namely area, barrier, and point coverage, are discussed in the literature. Simplified models based on Cassini ovals are used to evaluate two-dimensional bistatic and multistatic sonar coverage in a homogeneous environment where practical acoustic propagation characteristics such as spatial absorption loss, sound propagation pattern, shadow zones, and sound gradient effects are ignored [18], [19], [20], [21], [22]. The Cassini oval model has been used for scientific purposes to ease geometrical calculations in underwater sonar coverage studies. Additionally, another acoustic-based method used in MSSN coverage studies is the traditional sonar detection model, which is used with the assumption of the *TL* (Transmission Loss) model, where transmission loss is based on basic propagation geometry. When the studies in which the sonar detection model is used are examined, it is seen that the sound propagation model, shadow regions, and sound velocity profile effects, which are important in modeling the real underwater environment, are not considered. These analyses are also performed in two dimensions, assuming the spreading factor is a constant value [23], [24].

Sonar system detection performance in the underwater environment relies strongly on the relative locations of the source, receiver, and target, as well as ambient conditions [25], [26]. In addition, acoustic wave propagation patterns and depth-dependent sound velocity profiles are important factors in finding the correct detection range and coverage underwater [27]. For this reason, the accuracy of underwater target detection using sonar technology is determined by a wide range of environmental criteria used in acoustic ray tracing-based sonar performance prediction tools [28], [29]. In this way, ray trace-based propagation properties are simulated at different intervals and depths.

In this paper, a practical MSSN channel model has been proposed for the MSSN link budget, which includes underwater acoustic propagation parameters such as spectral variation of the absorption loss, ambient noise, sound speed profile, and the impact of shadow zones. In the practical MSSN channel model, in the calculation of propagation loss, the sound velocity profile, and the shadow zone effect are considered, the m parameter is corrected and our model is evaluated by Lybin, a well-known sonar performance prediction tool. In this way, besides the detection of shadow zones formed by the effect of the sound velocity gradient, the correct detection range is obtained by finding the actual spreading conditions, and the proper placement for real sonar scenarios is found. To the best of the authors' knowledge, this is the first study to examine the three-dimensional volume coverage problem in MSSN with realistic assumptions such as sound propagation and velocity profile varying with depth. Since the coverage analyses in MSSN so far have been done in two dimensions, it is very important to perform the analyzes in three-dimensions with the concept of volume coverage to get maritime safety

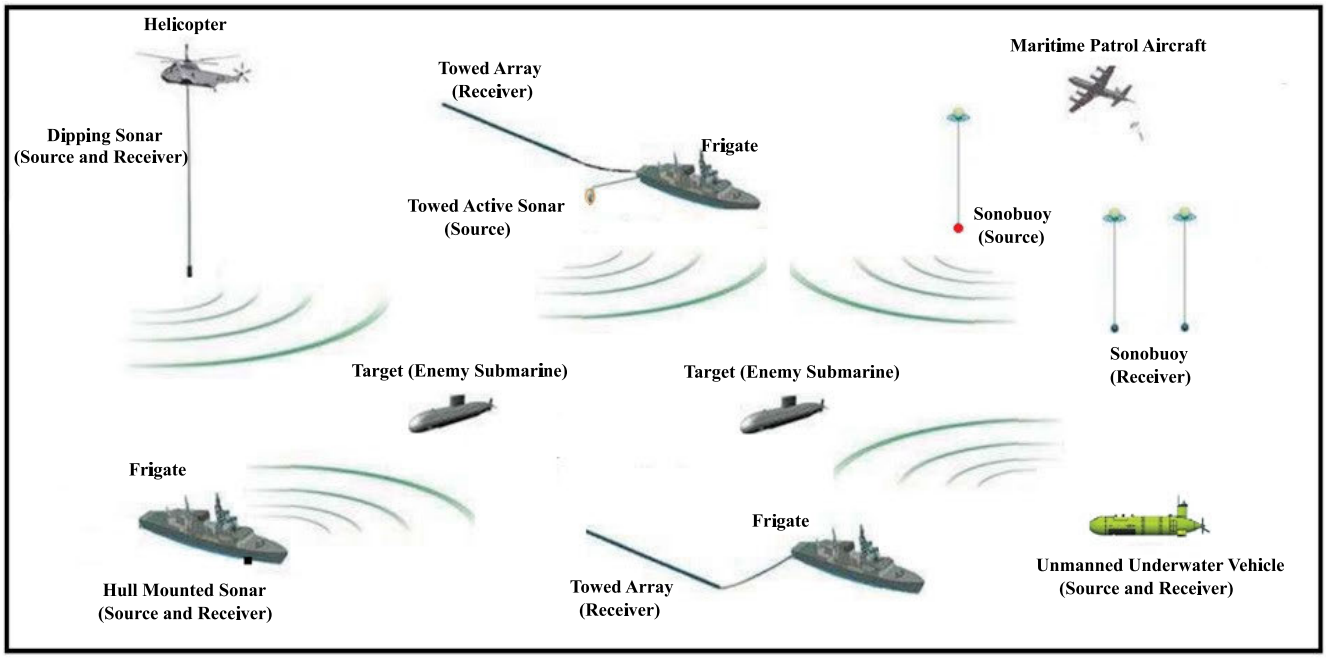

FIGURE 2. Illustration of the possible components of multistatic sonar systems.

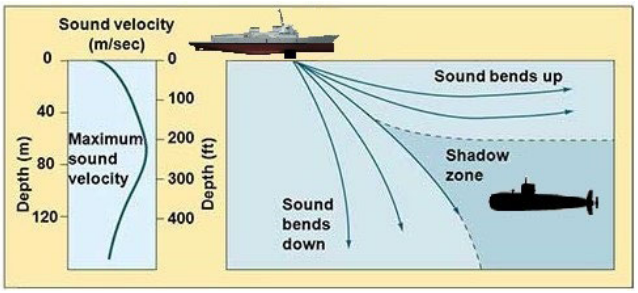

FIGURE 3. Sound propagation dependent on sound speed profile-shadow zone.

and underwater situational awareness. As shown in Fig. 3, hostile targets may hide in shadow zones with low sound intensity where acoustic waves emanating from a source cannot reach due to refraction [30]. Thus, it is critical to place the sensors to achieve full coverage in three dimensions with realistic parameters and assumptions in order to satisfy the accuracy requirements of the MSSN in terms of situational awareness in the oceans.

The main contributions of the paper are summarized as follows:

1) A practical three-dimensional channel model is proposed for the MSSN link budget that covers the frequency-dependent and realistic features of the underwater acoustic environment, such as the effects of sound propagation according to real ambient conditions.
2) The practical MSSN channel model is evaluated for the detection range dependent on ambient conditions using Lybin, a well-known sonar performance prediction tool. In this way, besides the detection of shadow zones formed by the effect of the sound velocity gradient, the correct detection range is obtained by finding the realistic spreading conditions, and the proper placement for real sonar scenarios is found.
3) Using the proposed channel model, the coverage problem in a three-dimensional MSSN volume is analyzed according to the acoustic transmission frequency, the distance between the source and receiver, and the source level. The result of the analysis calculates the number of source-receiver pairs to be used to cover a given MSSN volume for various model parameter settings.
4) The results obtained are compared with the Cassini oval and sonar detection models frequently used in previous MSSN coverage studies, via a volume error expression. The results reveal limitations on the applicability of the Cassini oval and traditional sonar detection models, depending on the frequency and environmental conditions, in realistic MSSN deployment scenarios.

The organization of the paper is as follows. Section II provides a summary of related work on sensor placement and coverage solutions. Section III presents some preliminaries on the underwater acoustic model and Section IV shows the Cassini oval model. In Section V, details the practical MSSN channel model. The analysis and results of the different models are presented in Section VI, and the outcomes of the analysis are discussed in Section VII. Section VIII concludes the paper with a summary of the study and possible future work.

II. RELATED WORK

Three main categories of sensing coverage exist: area coverage, barrier coverage, and point coverage [31]. The area coverage problem is related to the maximization of the sensing region. The objective of barrier coverage is to guarantee the sensing along a belt area or a line segment separating two areas. Point coverage aims to achieve the sensing of a set of points across the network region, such as patrol vessels. This section provides a detailed literature survey related to the coverage problem in MSSN.

In [23] and [24], the SCOUT program is used to improve area coverage. The placement of sensors and ping time scheduling are studied for multistatic active sonobuoys in a littoral environment. All analyses are performed in two dimensions, without a precise model of underwater acoustic propagation characteristics using the traditional sonar detection model.

Particle swarm optimization is utilized in [32] to find the optimal position, quantity, and type of multistatic sonar units to maximize area coverage. Two-dimensional analyses are performed using the Cassini oval model under the assumption of a homogeneous environment.

Cost-effectiveness conditions, detection probability models, placement of source-receiver pairs and impacts of sensor geometry on MSSN area coverage are also investigated in [20], [33], [34], and [35]. Sources, receivers, and targets are all positioned in two-dimensional space, and the Cassini oval model is used in these studies.

In [21] and [22], analytical methods are exploited to measure the effectiveness of randomly deployed multistatic sensors to provide the highest area coverage, considering the number of sensors, field width, and sensing range accounts. Two-dimensional analyses are performed using the Cassini oval model under the assumption of a homogeneous environment.

Mathematical models are proposed in [36] to determine the minimum cost of sensor placement with sufficient detection probability. Again, two-dimensional analyses are carried out, neglecting the adverse effects of the underwater acoustic propagation environment.

Various algorithms have been developed to provide the maximum point coverage to protect MSSN from hostile underwater assets [35], [37], [38], [39], [40], [41]. The algorithms aim at the optimal placement of a single source. A two-dimensional operating region with homogeneous environmental conditions is assumed, and the Cassini oval model is used.

Numerous algorithms developed for point coverage in a two-dimensional area are compared in terms of computation time and performance using the Cassini oval model in [42].

A hybrid point and barrier coverage application is examined in [43], [44], and [45]. The results obtained from the different algorithms are compared in terms of computational load and performance. None of these algorithms, which are investigated in a two-dimensional environment, take practical underwater acoustic channel characteristics into account.

Related studies on the solutions to the coverage problem in MSSN are summarized in Table 1. To the best of the author's knowledge, practical underwater acoustic propagation parameters such as spectral change of absorption loss, ambient noise, sound propagation, variation of the sound speed profile, and impact of shadow zones are exactly not modeled in any of these studies. Moreover, no three-dimensional analysis has been performed in the MSSN coverage studies. The concept of volume coverage is crucial to get maritime safety and underwater situational awareness. Hostile targets can be anywhere and placed at different depths of the ocean. Thus, we focus on MSSN's volume coverage in this study. The placement of a source and a receiver to cover a given three-dimensional ocean volume, which includes hostile targets, is our primary concern.

III. PRELIMINARIES

MSSN is based on the principle that the acoustic source signal reflected from the target is detected by the receivers in the network. Detection of the reflected signal is determined by the following sonar equation [46]:

$$SE = SL + TS - TL_{st} - TL_{tr} - NL + DI - DT \quad (1)$$

where SL is the source level, TS is the target strength, TL_{st} is the transmission loss from the source to the target, TL_{tr} is the transmission loss from the target to the receiver. NL is represents the ambient noise level. DI stands for the directivity index. DT is the detection threshold and SE is the signal excess value [47].

The source level of an underwater acoustic transmitter is given by

$$SL(P_t) = 170.8 + 10\log(\eta P_t) + DI \quad (2)$$

where P_t is the electrical input power in Watts, DI is the source directivity in dB, and SL is in dB re 1 μPa at 1 m. The electro-acoustic power conversion efficiency η for conventional sonar transmitters varies between 20% and 70% [48].

TS is the echo returned by an undersea target, such as submarines and torpedoes. It is related to the combination of the size, form, frequency, and aspect angles of the target. The suggested TS values for sonar system design and performance calculations are listed Table 2 [49] and the variation of the TS of a submarine with respect to the aspect direction is illustrated in Fig. 4 [50].

TL is a parameter used to describe the effect that results from the propagation and attenuation of sound intensity as the sound propagates through the ocean. The ratio of the sound intensity at 1 m from a source to the sound intensity at distance R is known as transmission loss. Oceanographic features of the underwater environment are among the factors affecting TL. TL consists of two factors, propagation loss, and absorption loss, and is modeled as follows [51]:

$$TL(D, f) = m\log(D) + \alpha(f)D10^{-3} \quad (3)$$

TABLE 1. Summary of related works.

Study	Objective	Coverage Type	MSSN Architecture	Reference Model	Method/Developed Algorithm
[20]	Studying study cost-effectiveness issues and the advisability of using co-located source/receiver pairs instead of independent sources and receivers	Area Coverage	2D	Cassini oval	Analytical model based on Cassini oval and Poisson Fields
[21]	Investigating pattern optimization, cost-effectiveness, reliability, and the relative attractiveness of multistatic versus monostatic systems for randomly placed sources and receivers on MSSN	Area Coverage	2D	Cassini oval	Multistatic search theory has been formulated for different conditions.
[22]	Determining the effectiveness of multistatic sonar systems, considering the receiver-source number, field width, and detection distance parameters, determining the optimum field width at which sensors should be used in order to provide the highest coverage	Area Coverage	2D	Cassini oval	Analytical theory based on Cassini ovals and Poisson Fields
[23]	Optimizing the sensor locations and ping times of multistatic active sonobuoys with the SCOUT program based on a genetic algorithm	Area Coverage	2D	Sonar detection	The ORP Search-Path Algorithm in the SCOUT program
[24]	Finding optimal solutions allowing resource control while preserving and maximizing performance for multistatic active sonobuoys in simulated non-homogeneous areas	Area Coverage	2D	Sonar detection	Updated SCOUT program with genetic algorithm solutions
[32]	Determining the optimum number and placement of multistatic sonar sensors to achieve maximum coverage while minimizing the number of sensors required with a PSO-based model	Area Coverage	2D	Cassini oval	Sequential PSO Algorithm
[33]	Performing analyses with sensor detection models in order to show the differences of multistatic systems compared to monostatic systems	Area Coverage	2D	Cassini oval	Analytical model based on Cassini ovals- monostatic and multistatic detection model
[34]	Obtaining the best placement geometry of bistatic sonobuoys when searching for stationary and moving targets for maximizing the target detection probability	Area Coverage	2D	Cassini oval	Analytical model based on Cassini ovals and Poisson Fields
[35]	To achieve maximum coverage, placement of a single source sensor for sensors with known receiver placements and investigating the effect of random and polygonal placement of receivers for different conditions.	Area Coverage	2D	Cassini oval	Analytical model based on Cassini oval (Effective Area Coverage)
[36]	Performing sensor placement optimization to find the lowest cost multistatic network that can cover all desired areas	Area Coverage	2D	Non-acoustic	INP, Standart Linearization, Glover's Linearization, Oral–Kettani's Linearization
[37]	Developing an algorithm that quickly provides optimum source location in terms of optimal placement of single source and sources for fixed receiver and target	Point Coverage	2D	Cassini oval	DIBS Algorithm
[38]	Obtaining optimal sensor locations using Detection Disk and RoD models for fixed receiver and target with improved computation time	Point Coverage	2D	Cassini oval	LOC GEN2 Algorithm
[39]	Studying the optimal placement of a fixed single source and fixed location with fixed targets and sensors to successfully detect the submarine threat in terms of point coverage.	Point Coverage	2D	Cassini oval	Convex Hull Based NLP, INLP and DIBS Algorithm
[40]	Single source sensor placement for sensors with known receiver locations to provide the highest coverage, and examining the effect of random and polygonal placement of receiver sensors on coverage for different scenarios.	Point Coverage	2D	Cassini oval	Point Coverage Model:OPT LOC Algorithm, GREEDY-LOC-DEF Algorithm
[41]	Modeling the best placement of the fixed source in terms of point coverage while the target and receivers are fixed, and presenting the performance of different algorithms in the literature and the results in terms of computation time comparatively	Point Coverage	2D	Cassini oval	LOC GEN, OPT LOC, GREEDY-LOC
[42]	Providing the highest coverage by placing both source and receivers together for fixed targets and evaluating different developed algorithms in terms of performance and computation time	Point Coverage	2D	Cassini oval	DISC-LOC-M, DISC-LOC-enum, Adapt-LOC, Iter-LOC, C&K Algorithm
[43]	Analyzing a hybrid point and barrier coverage application in which a decision-maker aims to position sensors along a two-dimensional belt-shaped barrier region	Barrier/Point Coverage	2D	Non-acoustic	ILP Model, INLP Model, GA Model
[44]	Addressing a two-level location problem with arrows within the scope of point and barrier coverage to improve coverage performance	Barrier/Point Coverage	2D	Non-acoustic	NSGA-II Algorithm
[45]	Examing the challenge of identifying along a two-dimensional belt-shaped border area including a number of key facilities requiring intruder protection	Barrier/Point Coverage	2D	Non-acoustic	HubsSpoke Topology: MINLP Model, MILP Model

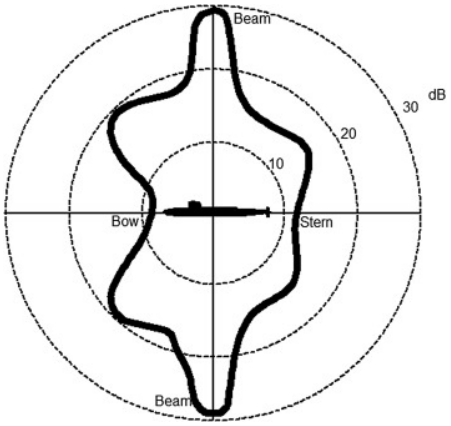

FIGURE 4. The variation of the *TS* of a submarine with respect to the aspect direction (butterfly shape).

m in (3) denotes the spreading factor for propagation loss term and α(f) represents the absorption coefficient for absorption loss term. The spreading factor m is generally assumed to be 10 for cylindrical propagation, 20 for spherical propagation, and 15 for practical sonar applications [52], [53].

The traditional sonar detection model is not concerned with the exact value of the m parameter, so the detection can lead to seriously erroneous results in terms of detection range and coverage. The absorption coefficient is expressed in dB/km using the empirical Thorp expression for f in kHz. The expression is valid for frequencies between 100 Hz and 1 MHz in units of dB/km for seawater with a salinity of 35 parts per thousand, a pH of 8, a temperature of 4 degrees Celsius, and a depth of 0 meters (atmospheric pressure) [52]:

$$\alpha(f) = \frac{0.11f^2}{1+f^2} + \frac{44f^2}{4100+f^2} + 2.75 \times 10^{-4} f^2 + 0.0033 \tag{4}$$

DT and signal-to-noise ratio (SNR) are related to the probability of detection. The difference between these two quantities is called Signal Excess (SE) [54]. Successful detection of a target requires the SE to be greater than 0 dB.

IV. CASSINI OVAL MODEL

A Cassini oval is a quartic plane curve for which the loci of points in the plane are determined by the constant product of the distances to two fixed foci. Applications such as

TABLE 2. Practical target strength value for submarines.

Aspect	Small	Large: clad	Large
Beam	5 dB	10 dB	25 dB
Intermediate	3 dB	8 dB	15 dB
Bow/stern	0 dB	5 dB	10 dB

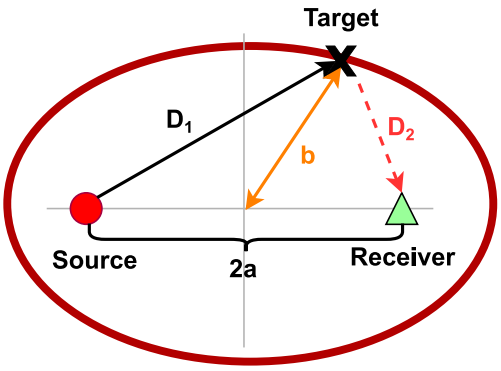

FIGURE 5. Source-Receiver-Target Triangle.

new generation bistatic radar and sonar systems, modeling of human red blood cells, simulation of light scattering are some of the areas where cassini ovals are used in the literature [55], [56]. In the Cassini oval model, the sonar equation is simplified by ignoring the spectral variation of the acoustic absorption and noise level. Consequently, the transmission loss follows the basic power rule for a constant $m > 0$ in a homogeneous medium with spherical spreading ($m = 20$) [18], [22], [34]. Thus, the condition for the detecting the reflected acoustic signal is

$$SL - m\log(D_1) - m\log(D_2) \geq NL - TS - DI + DT \quad (5)$$

As seen in Fig. 5, where D_1 and D_2 are the distances from the source to the target and from the target to the receiver, respectively. If (5) is solved for the product of bistatic distances, it can be seen in (6) that this product must be below a threshold value denoted as b^2:

$$D_1 D_2 \leq 10^{\left(\frac{SL-NL-TS-DI+DT}{20}\right)} \equiv b^2 \quad (6)$$

The above parameter b gives the equivalent monostatic sensing distance when the source and receiver are colocated. Equation (6) is the Cassini oval equation, which is used to figure out the target detection area of a bistatic/multistatic system [57]. According to the source-receiver-target triangle in Fig. 5, b is the constant indicating the monostatic sensing distance. D_1 and D_2 are seen as the sides of the triangle near the vertex, and the distance between the source and the receiver is defined as the length of the other side of the triangle [34]. The Cassini ovals are defined as follows the source and receiver are colocated at $(a, 0)$ [58]:

$$[(x-a)^2 + y^2][(x+a)^2 + y^2] = b^4 \quad a, b \in \mathbb{R} \quad (7)$$

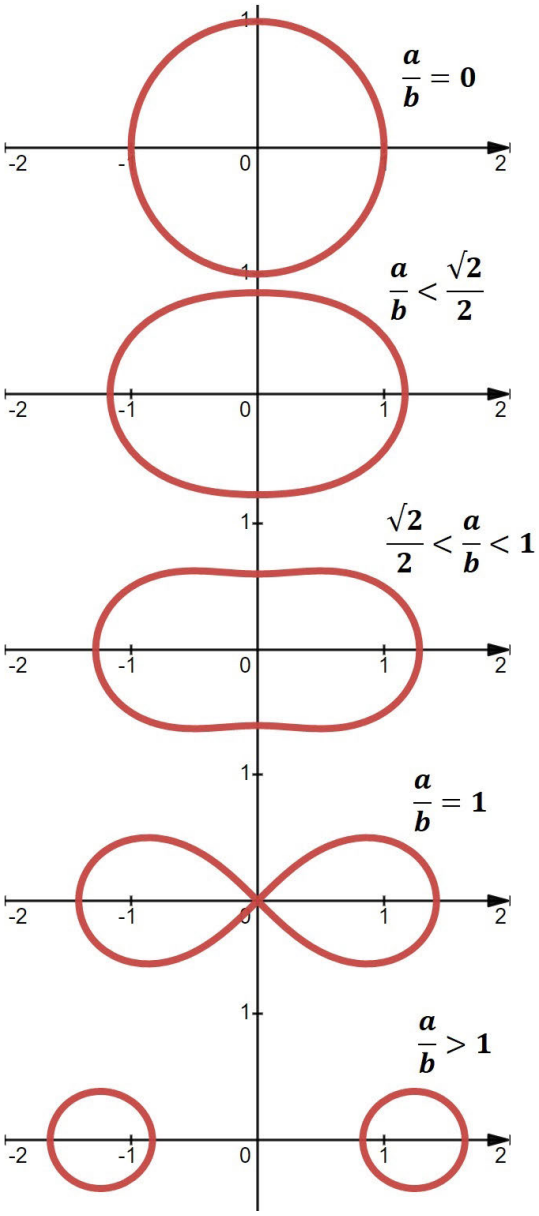

FIGURE 6. A family of Cassini oval for b = 1.

This oval is symmetrical about the x and y axes and its shapes change depending on the ratio of the basic parameters a and b.

- For $\frac{a}{b} \leq \frac{\sqrt{2}}{2}$ the curve is a single ellipse-shaped loop that intersects the x-axis at $x = \pm\sqrt{a^2 + b^2}$.
- For $\frac{\sqrt{2}}{2} \leq \frac{a}{b} \leq 1$ the figure somewhat inward from the top and bottom is in the shape of a non-convex curve.
- For $\frac{a}{b} = 1$ the figure is a Bernoulli Lemniscate. This curve passes through the center of the Cartesian plane and resembles the symbol ∞.
- For $\frac{a}{b} > 1$ the figure splits into two separate convex ovals and also intersects the x-axis at $x = \pm\sqrt{a^2 - b^2}$

Fig. 6 shows the possible shapes for different conditions on a for $b = 1$.

Reference Model	Traditional Sonar Detection Model	Cassini Oval Model	Practical MSSN Channel Model
Architecture in MSSN Coverage Studies	2D	2D	2D 3D
Effect of Sound Speed Profile and Shadow Zone	X	X	✓
Effect of Absorption Coefficient	✓	X	✓
Effect of Propagation Spreading Factor	✓ $m = 15$ (Practical spreading factor)	✓ $m = 20$ (Spherical spreading factor)	✓ Obtained from Lybin according to real ambient conditions

V. PRACTICAL MSSN CHANNEL MODEL

In the MSSN coverage analysis studies carried out in the literature, it was determined that the coverage analyses were performed in two dimensions, and the Cassini oval and traditional sonar detection models used in the analyses were insufficient in terms of realistic underwater modeling. Therefore, a practical MSSN three-dimensional channel model is proposed, and the model depends on actual detection ranges depending on ambient conditions using the sonar performance prediction tool. The differences between the models previously used in MSSN coverage studies and the practical MSSN channel model are summarized in Table 3 in terms of some realistic features of the underwater acoustic environment.

A. NETWORK MODEL AND ASSUMPTIONS

The objective of our model is the placement of source-receiver pairs for maximum coverage of possible target locations in a three-dimensional MSSN volume. Our assumptions can be summarized as follows:

- Source and receiver sensors are deployed at any desired location in accordance with the bottom grid deployment scenario. The use of sonobuoys gave rise to the idea of an easily deployable sonar system that can work with depth control [59].
- Sensors have a spherical communication range D, which is determined by the frequency of the acoustic signals. The effects of frequency, source level, and the distance between the source and the receiver are taken into account.
- The target is assumed to be a large-sized submarine, and average signal reflection is assumed to emanate from the intermediate aspect of the target.
- The environment is assumed homogeneous. The sound speed profile is modeled and as constant $c = 1500$ m/s with a depth gradient in underwater acoustic propagation.
- A realistic assumption is used for the spreading loss. It is determined according to the well-known sonar performance modeling tool Lybin [60].
- Sources and receivers are omnidirectional, hence $DI = 0$ dB.
- Cookie cutter model is used as the target detection criterion. When a target enters the detection range, of a sensor ($SE = 0$), the target will be detected.

B. PROBLEM FORMULATION

In previous studies on MSSN coverage using the Cassini oval model, the frequency dependence of the absorption coefficient is ignored and only a spherical spread is assumed. On the other hand, in the sonar detection model, which is another model used in MSSN coverage studies, the m parameter is accepted as a constant value, and the analysis is carried out under the assumption of a practical spreading factor $m = 15$. Sound propagation in the underwater environment may vary depending on the oceanographic environment conditions. Sonar system detection performance in the underwater environment is highly dependent on ambient conditions and the relative positions of the source, receiver, and target. The change in the speed of sound, and the surface and bottom boundary conditions of the ocean severely affect the propagation of sound. Therefore, it is important to accurately model the transmission loss in the underwater acoustic environment to include ray tracing theory and depth-dependent sound velocity profile parameters in sonar performance modeling to obtain the true detection range and coverage. From this point of view, in our practical MSSN channel model, in the calculation of the TL propagation loss parameter, the sound velocity profile, and the shadow zone effect are considered, and the m parameter is corrected. Our model is evaluated by Lybin sonar performance modeling tool.

One of the most important factors for detection range calculations in sonar systems is frequency-dependent sea ambient noise levels. The main parameters affecting the sea ambient noise model are water turbulence N_t, shipping noise N_s, thermal noise N_{th} and wind noise N_w. These parameters can be modeled using Gaussian statistics and power spectral density (PSD) in dB re $\mu\ Pa^2$ per Hz.

$$NL(f) = N_t(f) + N_s(f) + N_{th}(f) + N_w(f) \tag{8}$$

Turbulence Noise: Turbulence-induced noise emerges because of non-linear interactions by the ocean surface waves produced by the wind and wind generated as a result of ship movement. Flow noise from turbulence is a low-frequency phenomenon that predominates in the 1-100 Hz band. Turbulence-induced noise depends on ambient noise measurements, turbulence intensity, and transducer geometry, and is expressed as [61]:

$$N_t(f) = 17 - 30\log f \tag{9}$$

TABLE 3. Sea state, wave and wind speed.

Sea State	0	1	2	3	4	5	6
Wind Speed (Knots)	<1	5	13	16	19	22	28
Wave Height (m)	0	0.05	0.4	0.7	1.3	2	3

Shipping Noise: Shipping noise refers to the impact of a ship's machinery, propeller motion, and ocean traffic on the ambient frequency and shipping density (s) and it is defined as follows [62]:

$$N_s(f) = 40 + 20(s - 0.5) + \log \frac{f^{26}}{(f + 0.03)^{60}} \quad (10)$$

The value of s varies between 0 and 1, representing high and low activity, respectively. Shipping noise is the main source of ambient noise in the distribution of shipping routes in the oceans, port entrances, and shallow water areas with heavy ship traffic. However, at long distances, the primary source of ambient noise appears to be wind noise rather than shipping noise [62].

Thermal Noise: The molecular agitation of the water causes thermal noise, which is frequency-dependent. Above 100 kHz, thermal noise predominates and is defined as follows [62].

$$N_{th}(f) = -15 + 20 \log f \quad (11)$$

Wind Noise: Wind noise is caused by the interaction of many factors, including surface waves, water droplets, and bubbles from breaking waves [63]. The amount of ambient noise is significantly influenced by wind noise. Over the frequency range of 100 Hz to 100 kHz, ambient noise depends on changing wind speed (w) in meters per second. Wind noise can be calculated as follows [51]:

$$N_w(f) = 50 + 7.5\sqrt{w} + 20 \log f - 40 \log(f + 0.4) \quad (12)$$

The values used in practical sonar calculations for the sea state, wave height, and wind speed are listed in Table 3 [49].

The practical spectrum values of the ambient noise obtained in [64] are summarized in Fig. 7.

The above equation shows that neglecting the frequency dependence of the underwater acoustic ambient noise yields inaccurate results in terms of the target detection range and MSSN coverage. Therefore, as for the absorption coefficient, we use the spectral variation of ambient noise in our practical MSSN channel model. To obtain three-dimensional volume coverage with our model, the operating frequency of the multistatic sonar system, the distance between the source and the receiver, and the source level values must be determined. The effect of these values will be examined in detail in Section VI.

The procedure for calculating the three-dimensional volume and the minimum number of source-receiver pairs required to cover volume V is summarized in Algorithm 1. The following steps, which correspond to the lines in

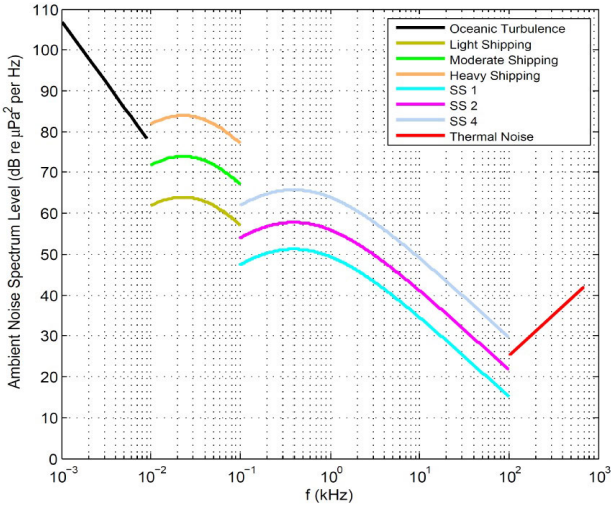

FIGURE 7. Frequency dependent ocean ambient noise.

Algorithm 1, can be used to summarize the method:

$$\begin{aligned} T(x,y,z) &= \bigcup_{i=1}^{n} T_i(x,y,z) \\ \text{s.t. } SE &= 0 \\ SE &= SL + TS - TL_{st}(D_1,\alpha) \\ &\quad -TL_{tr}(D_2,\alpha) - NL + DI \quad (13) \\ D_1 &= \sqrt{(Sx-Tx)^2 + (Sy-Ty)^2 + (Sz-Tz)^2} \\ D_2 &= \sqrt{(Tx-Rx)^2 + (Ty-Ry)^2 + (Tz-Rz)^2} \\ V_{SL,f,D_{s-r}} &= \pi \int_a^b T(x,y,z)^2 \quad (14) \\ n_{srpair} &= \frac{V_{SL,f,D_{s-r}}}{V_{total}} \quad (15) \end{aligned}$$

Algorithm 1 Practical MSSN Channel Model

(1) Initialize MSSN Parameters:
SL (dB), TS (dB), NL (dB), DI (dB), DT (dB), SE (dB), f (Hz), D_{s-r} (m), S_{xyz} (m), R_{xyz} (m)
TL = CalculateTL(SL, TS, NL, DI, DT, SE)
(2) m Parameter Correction for Real Equivalent Detection Range and Evaluate the Model
$DetRange \leftarrow LybinSE = 0 \leftarrow TL$
$mnew$=TL2mcoef(TL,$DetRange$, α) ▷ (3)
(3) Getting Possible Target Set Points
$T(x,y,z)$ = GetPossibleTargetPoints(SE,D_{s-r},S_{xyz},R_{xyz}) ▷ (13)
(4) Obtaining 3D Volume Coverage from Possible Target Set
$V_{SL,f,D_{s-r}}$=GetVolume($T(x,y,z)$) ▷ (14)
(5) Finding the Number of Source-Receiver Pairs to Cover Volume
$Npairs$=GetNpairs($V_{SL,f,D_{s-r}}$, V_{total}) ▷ (15)

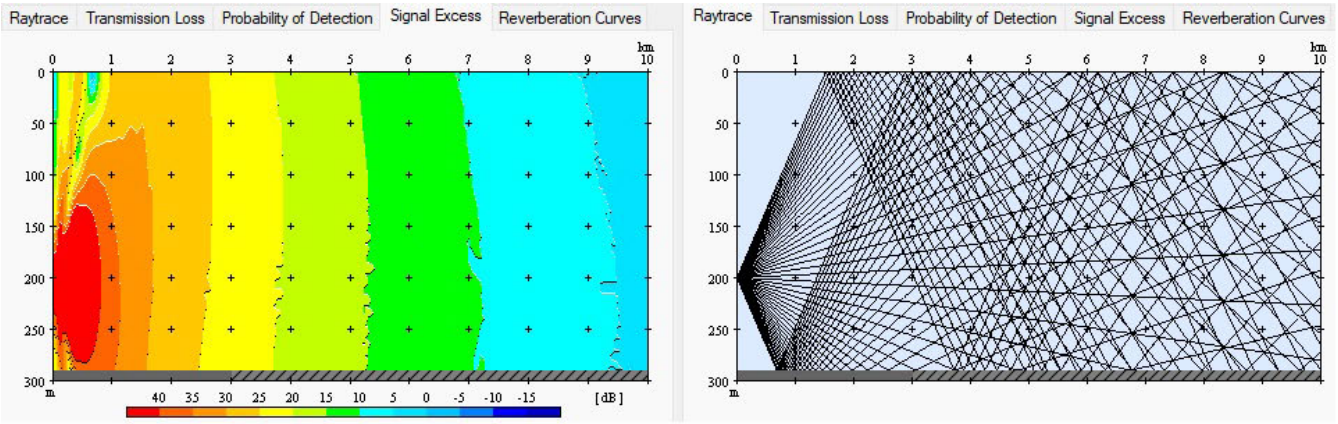

FIGURE 8. Lybin sample screen display.

Step 1 Initialize MSSN Parameters: Firstly, we initialize the sonar equation parameters in the constraint function in accordance with the practical MSSN channel model. The TL value is obtained by solving for $SE = 0$ function, which includes the sonar equation constraint functions. $SE \geq 0$ means that a target is successfully detected if the echo level of at least one receiver exceeds a certain level.

Step 2 m Parameter Correction for Real Equivalent Detection Range and Evaluate the Model: The propagation of sound is significantly impacted by changes in sound speed as well as ocean surface and bottom boundary conditions. In order to achieve the correct detection range and coverage, it is crucial to estimate the transmission loss in the underwater acoustic environment. The effect of the TL creates significant differences in target detection distances due to the cylindrical or spherical propagation of the sound. For this reason, the m value we mentioned earlier in (3), the correction is made for the obtained detection range value in accordance with the ambient conditions with the use of the Lybin sonar performance modeling tool which is a widely used and well-established range-dependent sonar prediction tool [60]. Lybin calculates the probability of detecting targets in underwater areas by using a broad set of element parameters that belong to the sonar systems, hostile targets, and environmental conditions such as sound speed profile, and ambient noise [65]. In the practical MSSN channel model algorithm, environmental condition parameters such as sound velocity profile and ambient noise, as well as initiated sonar parameter values are entered into the Lybin program, and analysis is run. Thus, the real equivalent detection range corresponding to the $SE = 0$, calculated in Step1, is obtained from the result of the analysis for which a sample screenshot is shown in Fig. 8. The real equivalent detection range value obtained as sample seen in Fig. 9 is substituted in (3) and the m absorption coefficient expression in our model is rearranged. Thus, our model is evaluated and corrected in terms of the detection range term with the help of the Lybin sonar performance modeling tool.

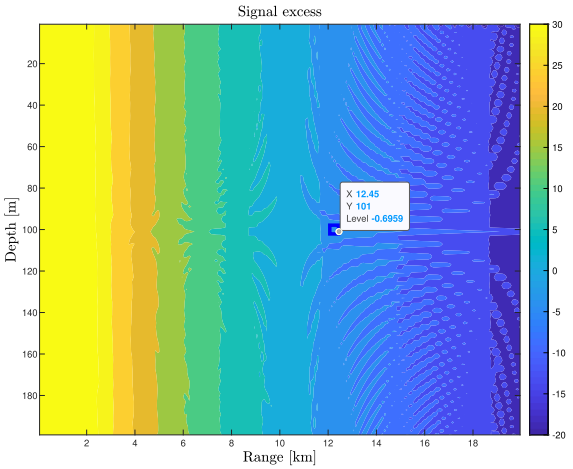

FIGURE 9. Sample figure of real detection range getting from Lybin for SE=0 condition ($f = 5$ kHz, $SL = 212$ dB, $D_{s-r} = 2000$ m).

Step 3 Getting Possible Target Set Points: In this step, the source and receiver are placed at a known fixed point. According to the practical MSSN channel model, as specified in (13), the set of possible target points for boundary values where the SE function is equal to zero as a reference cookie-cutter sensor model is obtained by the brute force method [66]. Pings are considered to be detected if the signal level listened by a receiver is above the detection threshold level. This level of signal is called SE and is considered sufficient to "detect" the target. Based on SE, the sensing curve of the sensor has the cookie-cutter pattern shape as shown in Fig. 10, which shows full detection in a certain range and no detection in a certain range. According to this model, the probability of detecting (PoD) a target using the source and receiver is as follows:

$$PoD = \begin{cases} 1, & \text{if } SE \geq 0 \\ 0, & \text{otherwise.} \end{cases} \tag{16}$$

Step 4 Obtaining 3D Volume Coverage from Possible Target Set: The boundary points of the set of possible target

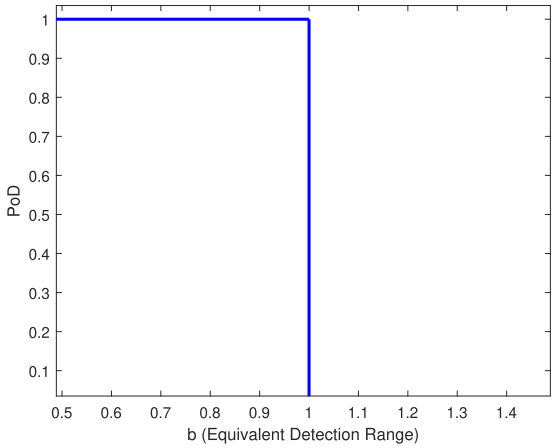

FIGURE 10. Cookie-Cutter Sensor Model [67].

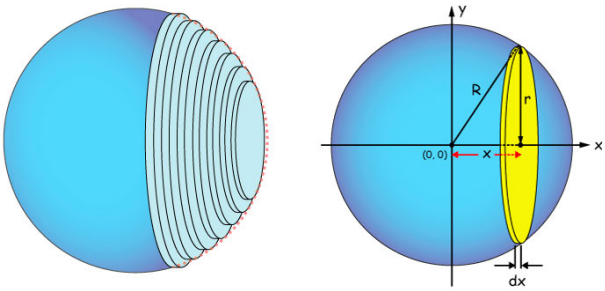

FIGURE 11. Volume calculation with the Disk method [67].

points obtained are rotated on the fixed axis and converted into the volume expression represented by the V expression using the disk method as seen in (14). The disk method is a technique for calculating the volume of an object by slicing it into many small cylinders or disks and then adding the volumes of all of these small disks, as shown in Fig. 11 [67], [68]. The volume is found by rotating the curve around the x-axis and y-axis.

Step 5 Finding the Number of Source-Receiver Pairs to Cover Volume: The number of source and receiver pairs required to guarantee full coverage of a given V volume is defined as (15), which is the ratio of the entire monitoring volume to the effective monitoring volume obtained for a source-receiver pair.

VI. NUMERICAL RESULTS

In this section, three-dimensional coverage for MSSN is studied for various operating frequencies, source-to-receiver distances, and SL values. The number of source-receiver pairs to guarantee volume coverage is calculated for each scenario and the results revealed by our practical MSSN channel model are compared with the number of sensor pairs obtained using the Cassini oval model and traditional sonar detection model as a volume error expression. The volume error expression can be calculated as (17):

$$E1 = \frac{V_{Cassini} - V_{MSSN}}{V_{MSSN}}, E2 = \frac{V_{SonarDet} - V_{MSSN}}{V_{MSSN}} \quad (17)$$

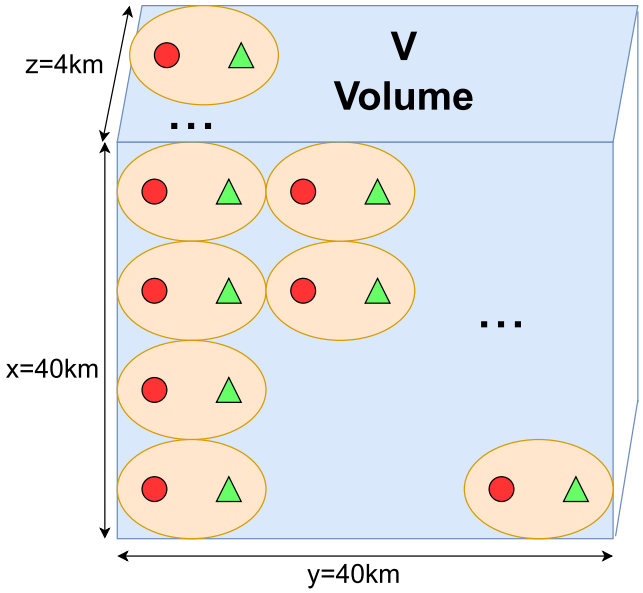

FIGURE 12. Deployment of source-receiver pairs for three-dimensional coverage in volume V.

The coverage problem is investigated within a volume V with dimensions of $40000 \times 40000 \times 4000m^3$, as shown in Fig. 12. We assume the sonar sensors are omnidirectional, hence DI is set to 0. The target is assumed to be a large-sized submarine, and the average signal reflection is assumed to emanate from the intermediate aspect of the target. Additionally, we assume a sonobuoy suitable for multistatic use in the market [69], as it can be deployed using the 3D bottom-grid strategy in order to suit a real sonar scenario. Regarding the ambient noise, moderate shipping is to have $s = 0.5$, and the wind influence on the MSSN channel model is accounted for with $w = 10$ m/s corresponding to sea state 4 for noise-limited scenarios. Table 4 displays the parameters used in our analysis.

A. EFFECT OF ACOUSTIC TRANSMISSION FREQUENCY

In this analysis, the effect of acoustic transmission frequency on MSSN coverage is examined for $SL = 212$ dB and $D_{s-r} = 2000$ m. The source (S_{xyz}) is located at (0, 0, 0) and the receiver (R_{xyz}) is at (0, 2000, 0).

In comparative analyses in this main section, the red circle, and the green triangle represent the source and receiver, respectively. Light blue lines around the source-receiver pair show the possible furthest target detection locations, which are obtained using our practical MSSN channel model. However, target positions in the maximum detection range provided by the Cassini oval model and traditional sonar detection model are represented by claret red dashed line marks and orange lines, respectively. Using the disk method explained in Section V, these points on the x-y plane are rotated to obtain the volume covered by the corresponding source-receiver pair. For readability and clarity purposes, the cross sections for the volumes along the x-y plane are shown in the figures.

TABLE 4. Parameter values.

Parameter	Values
SL (dB)	206...218
TS (dB)	15
f (Hz)	1000...50000
NL (dB)	depends on frequency
α (dB/km)	depends on frequency
T (°C)	14
P (atm)	1
Salinity (%)	35 ppt
Acidity (pH)	8
s	0.5
w (m/s)	10
DI (dB)	0
DT (dB)	0
Pulse Type	CW
PW (ms)	1000
m	Obtained from Lybin
D_{s-r} (m)	1000...12000
V (m^3)	40000x40000x4000

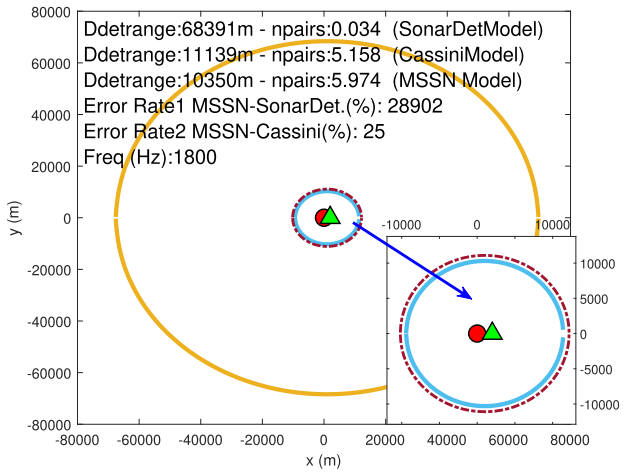

FIGURE 13. Comparative results for f = 1.8 kHz, SL = 212 dB, D_{s-r} = 2000 m.

Fig. 13 shows the results for $f = 1.8$ kHz. The detection ranges for the traditional sonar detection model, the Cassini oval model, and our MSSN channel model are 68391 m, 11139 m, and 10350 m, respectively. According to our model and the Cassini oval model, 6 source-receiver pairs must cover V, whereas 1 pair is sufficient according to the sonar detection model. Our model, which uses real environmental conditions and the sonar performance modeling tool to find the sonar detection distance, has an error rate of 25% between the Cassini oval model and around 28000% for the sonar detection model.

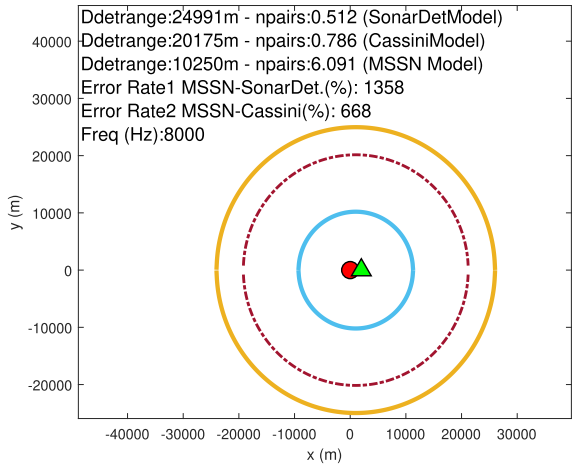

FIGURE 14. Comparative results for f = 8 kHz, SL = 212 dB, D_{s-r} = 2000 m.

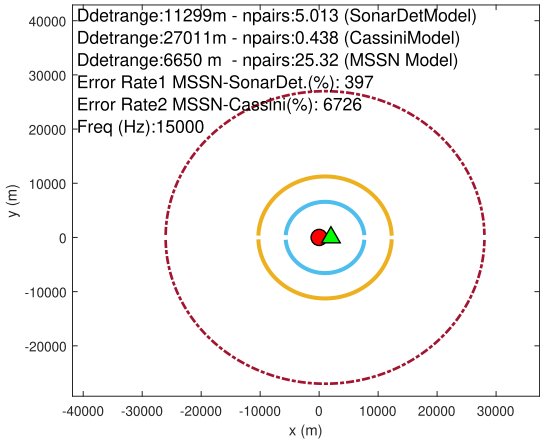

FIGURE 15. Comparative results for f = 15 kHz, SL = 212 dB, D_{s-r} = 2000 m.

When the frequency is increased to 8 kHz, according to the Cassini oval and sonar detection model requires 1 pair to cover volume V, which cannot be fully covered with less than 7 pairs for our MSSN channel model. As shown in Fig. 14, the difference is 600 percent for the MSSN channel model and Cassini oval model. Besides, the error rate between the MSSN channel model and sonar detection model is approximately 1300%.

Figs. 15 and 16 show the results obtained using the three models for $f = 15$ kHz and $f = 30$ kHz, respectively. Due to the nonlinear change in absorption and ambient noise with frequency, the target detection range decreases for our practical MSSN channel model and sonar detection model. However, the detection range for the Cassini oval model raises unexpectedly since the spectral effects are ignored.

Concerning the Cassini oval model, 1 pair are enough for $f = 15$ kHz and even 1 pair suffices for coverage at $f = 30$ kHz too. Additionally, according to the sonar detection model, 6 pairs are required for 15 kHz and 73 pairs for

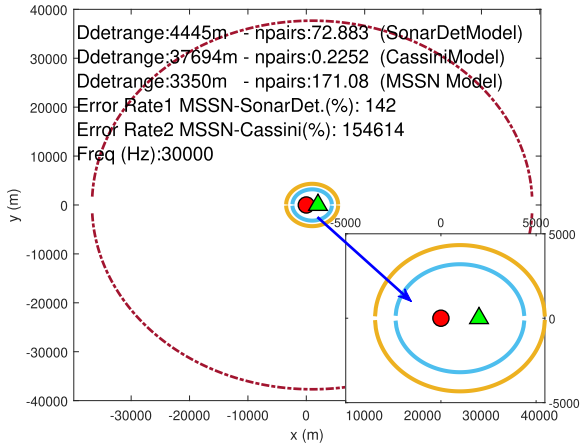

FIGURE 16. Comparative results for $f = 30$ kHz, $SL = 212$ dB, $D_{s-r} = 2000$ m.

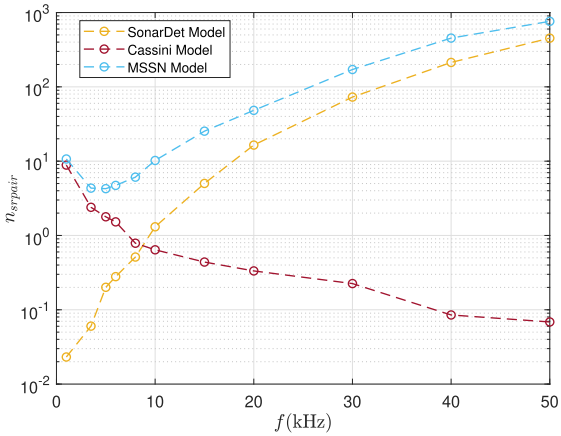

FIGURE 17. The required number of source-receiver pairs for the three models with respect to frequency ($SL = 212$ dB, $D_{s-r} = 2000$ m).

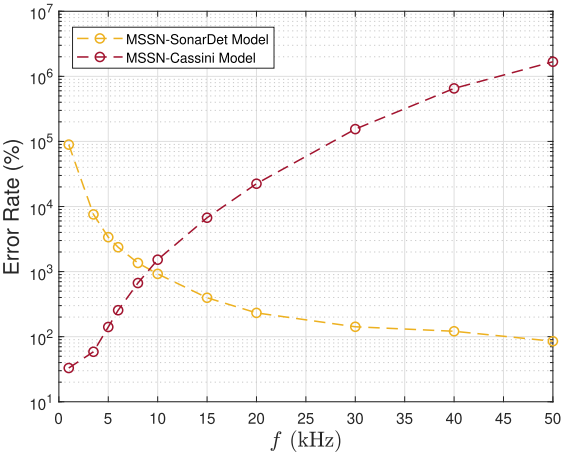

FIGURE 18. The difference between the results yielded by the models, which is a measure of the error in the calculation of the required number of pairs, against frequency ($SL = 212$ dB, $D_{s-r} = 2000$ m).

30 kHz in order to fully cover the V volume. According to our practical MSSN channel model, which is built on the spectral variation of the underwater acoustic propagation characteristics, we need 26 and 172 source-receiver pairs for coverage at 15 and 30 kHz, respectively. The required number of source-receiver pairs for the three models is compared in Fig. 17. The difference between the volume results yielded by the models, which is a measure of the error in the calculation of the required number of pairs, is plotted against frequency in Fig. 18. As Fig. 18 shows, serious error effects are observed between the models depending on the frequency.

Consequently, the number of pairs obtained from the Cassini oval model is much smaller than the actual number of pairs required for three-dimensional coverage, as given by our practical MSSN channel model and sonar detection model. However, the main reason for the difference between the sonar detection model and our MSSN channel model is the m spreading factor value. The sonar detection model accepts the spreading factor term as a constant value without considering the real environmental conditions, and at low frequencies, there is an enormous difference between our MSSN channel model and sonar detection model in terms of sonar detection distance since the absorption coefficient is not dominant.

B. EFFECT OF SOURCE LEVEL

This analysis examines the effect of SL on MSSN coverage based on frequency. For this reason, the analysis is performed at $D_{s-r} = 4000$ m for 2 different frequencies $f = 3500$ Hz and $f = 20000$ Hz. The location of the source (S_{xyz}) is (0, 0, 0), and the location of the receiver (R_{xyz}) is (0, 4000, 0).

The results for $f = 3500$ Hz and $SL = 206$ dB are shown in Fig. 19. The sonar detection model, the Cassini oval model, and our MSSN channel model have detection ranges of 43575 m, 10026 m, and 8650 m, respectively. Hence, in order to cover V, 1 source-receiver pair is required for the sonar detection model, 2 pairs for the Cassini oval model, and 3 pairs according to the MSSN channel model. The results obtained by the MSSN channel model and Cassini oval model differ by almost 60%. On the other hand, it is seen that there is 13000% difference between the MSSN channel model and sonar detection model.

When the SL increases to 212 dB, the detection range for the sonar detection model is 51538 m while that for the Cassini oval model is 14161 m. However, if the MSSN channel model, which considers the real environmental conditions, is used, the detection distance is 12150 m. As demonstrated in Fig. 20, the difference in volume coverage between the MSSN channel model and sonar detection model is 7650 percent here. The volume error rate between the MSSN channel model and Cassini model is around 60 percent.

Fig. 21 shows the results obtained using the three models for $f = 20$ kHz and $SL = 209$ dB. Regarding the sonar detection model and Cassini oval model, 5 source-receiver pairs and 1 pair are sufficient to guarantee V volume coverage, respectively. According to our practical MSSN channel model, we need 16 pairs to cover V. As shown in Fig. 21, the error difference between the MSSN channel model and sonar detection model, in this case, is almost 18000%. The

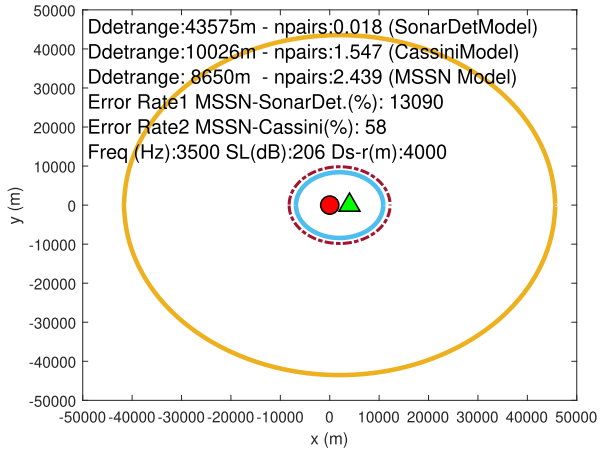

FIGURE 19. Comparative volume results for models under "$SL = 206$ dB, $f = 3.5$ kHz, $D_{s-r} = 4000$ m" conditions.

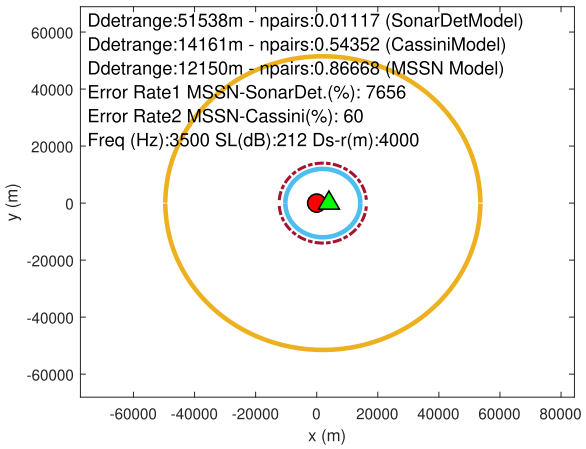

FIGURE 20. Comparative volume results for models under "$SL = 212$ dB, $f = 3.5$ kHz, $D_{s-r} = 4000$ m" conditions.

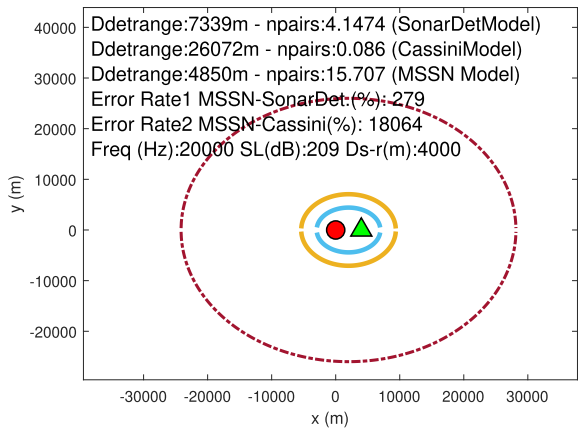

FIGURE 21. Comparative volume results for models under "$SL = 209$ dB, $f = 20$ kHz, $D_{s-r} = 4000$ m" conditions.

difference between the MSSN channel model and Cassini oval model is around 270 percent.

Looking at Fig. 22 for the $f = 20$ kHz and $SL = 215$ dB, 11 source-receiver pairs are needed to guarantee full coverage

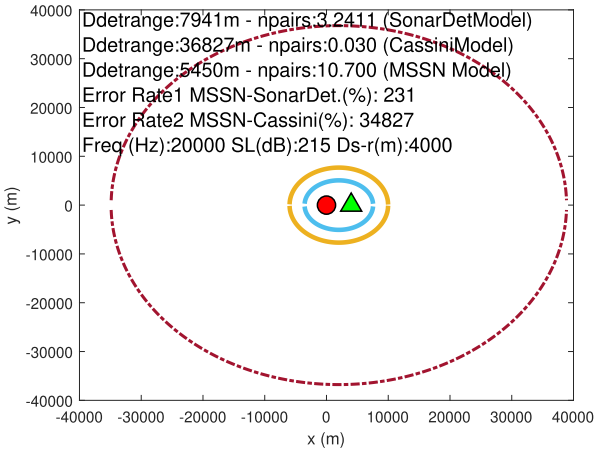

FIGURE 22. Comparative volume results for models under "$SL = 215$ dB, $f = 20$ kHz, $D_{s-r} = 4000$ m" conditions.

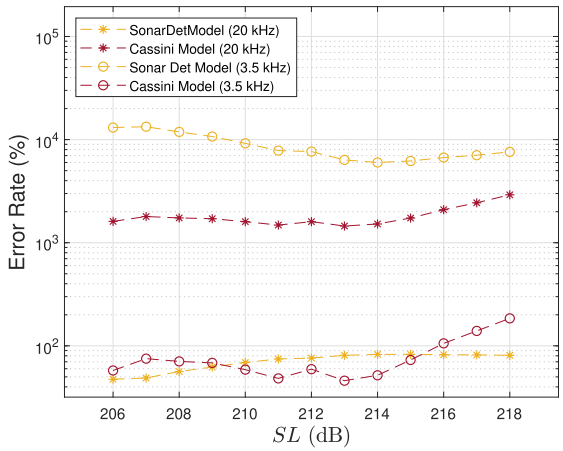

FIGURE 23. The difference between the results yielded by the models, which is a measure of the error in the calculation of the required number of pairs, against SL ($f = 3.5$-20 kHz, $D_{s-r} = 4000$ m).

using the MSSN channel model. Moreover, it is seen that the difference between the MSSN channel model and sonar detection model is around 230%, while the difference with the Cassini oval model has increased, even more, reaching 34000%.

It can be seen in Fig. 19-22 that as the SL value increases, the available target points obtained from the sonar detection model, the Cassini oval model, and MSSN channel model obtain a larger volume. In Fig. 23, the difference between the results produced by the models as a measure of the error in volume coverage is displayed versus SL for two different frequencies. It is seen that the error rate varies between the models much more with the effect of frequency, rather than the SL.

C. EFFECT OF SOURCE-TO-RECEIVER DISTANCE

This analysis investigates the effect of the distance between the source and receiver on MSSN coverage when $f = 15$ kHz and $SL = 212$ dB. Fig. 24 illustrates the results obtained

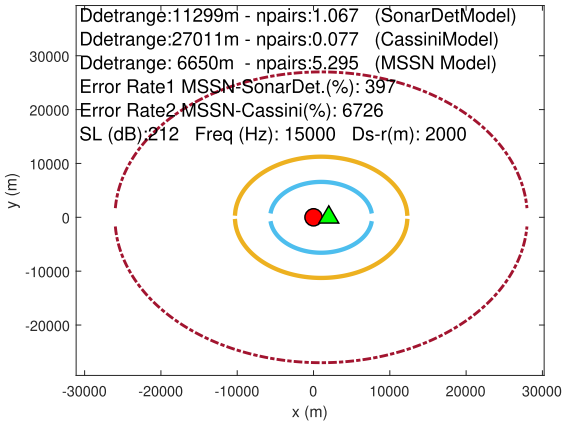

FIGURE 24. Comparative volume results for models under "D_{s-r} = 2000 m, SL = 212 dB, f = 15 kHz" conditions.

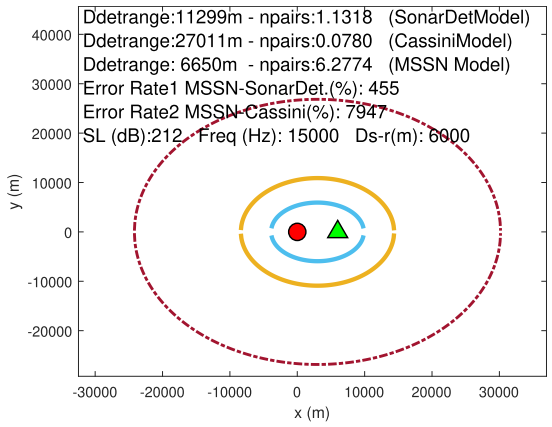

FIGURE 25. Comparative volume results for models under "D_{s-r} = 6000 m, SL = 212 dB, f = 15 kHz" conditions.

using the three models when $D_{s-r} = 2000$ m. Regarding the sonar detection model, 2 source-receiver pairs are adequate to achieve V volume coverage. According to the Cassini oval model, 1 source-receiver pair is adequate for coverage and our practical MSSN channel model shows that 6 pairs are required to cover V. The volume coverage error rate between the sonar detection and to MSSN channel model is approximately 400%. As for differences between Cassini and MSSN channel models is to around %6700.

When the distance between the source and receiver is increased to 6000 m, the MSSN channel model requires 7 pairs for the same volume V. As shown in Fig. 25, when the coverage volume of the sonar detection model and MSSN channel model are compared, it is seen that the error rate is close to 450 percent. The difference with the Cassini oval model is around 8000%.

The results for $D_{s-r} = 12000$ m are shown in Fig. 26. According to sonar detection model and Cassini oval model, 2 source-receiver pairs and 1 pair are required to cover V, respectively, whereas 19 pairs are according to our model. The results obtained by the Error rate1 differ by 1200%. The Error rate2 is around percent 23000.

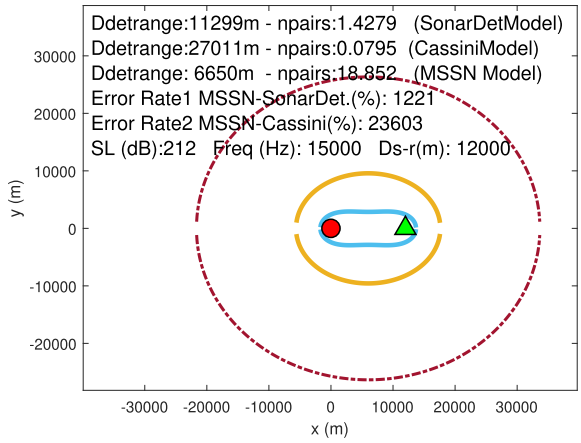

FIGURE 26. Comparative volume results for models under "D_{s-r} = 12000 m, SL = 212 dB, f = 15 kHz" conditions.

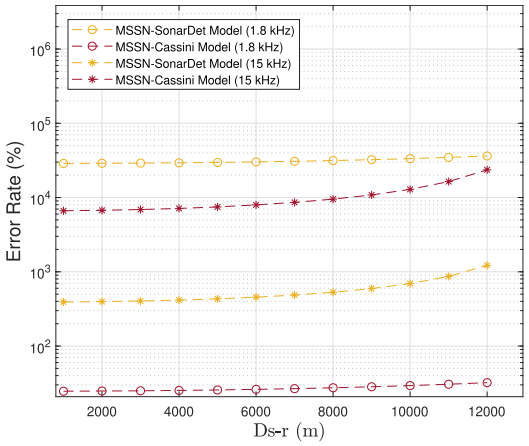

FIGURE 27. The difference between the results yielded by the models, which is a measure of the error in the calculation of the required number of pairs, against source-receiver distance (SL = 212 dB, f = 1.8-15 kHz).

As the distance between the source and receiver value grows, the potential target locations by models get a lower three-dimensional volume as seen in Fig. 24-26. In addition, in Fig. 27, the error rate between the three models depending on the distance between the source and receiver is expressed for two different frequencies as low and high. When Fig. 27 is examined, it is seen that as the distance between the source and receiver value increases, the error difference between the models increases, but the frequency effect is more dominant.

VII. DISCUSSION

This section summarizes the importance of the results of our analysis concerning MSSN deployment to achieve situational awareness in mission-critical applications.

The number of pairs required for three-dimensional coverage using the three models is plotted with respect to source level and frequency in Figs. 28-30. Additionally, variations of the target detection range for the models are shown in Figs. 31-33.

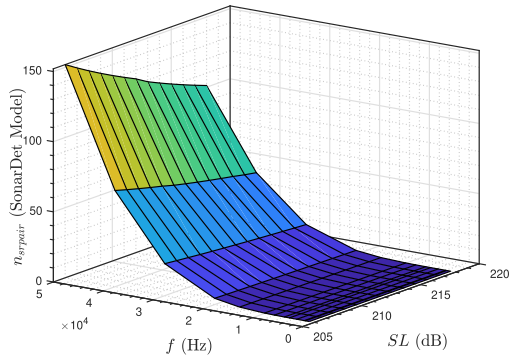

FIGURE 28. Number of pairs required for V coverage with respect to *SL* and *f* for $D_{s-r} = 2000$ m (Sonar detection model).

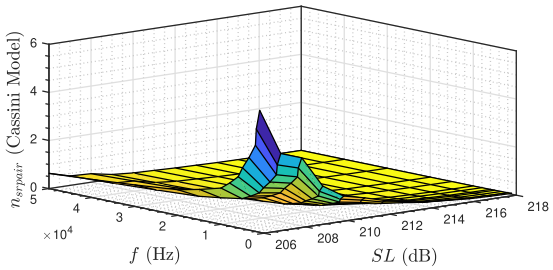

FIGURE 29. Number of pairs required for V coverage with respect to *SL* and *f* for $D_{s-r} = 2000$ m (Cassini oval model).

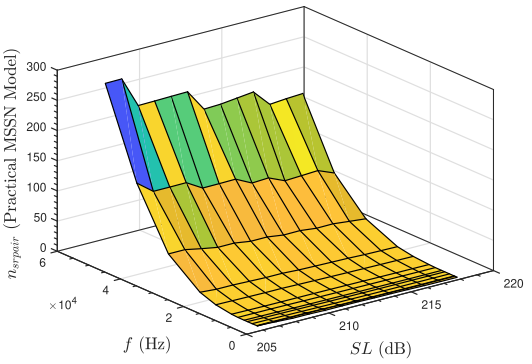

FIGURE 30. Number of pairs required for V coverage with respect to *SL* and *f* for $D_{s-r} = 2000$ m (Practical MSSN model).

When Figs. 28-33 are examined, some findings are as follows:

- The detection range obtained from the traditional sonar detection model continues to decrease depending on the frequency increase. Similarly, as the frequency increases, the number of source-receiver pairs required for full volume coverage with the sonar detection model increases.
- The detection range found using the Cassini oval model increases in parallel with the increase in frequency, unlike the sonar detection model. In addition, it is seen that the number of pairs to be used for full-volume coverage with the Cassini oval model decreases significantly depending on the frequency.

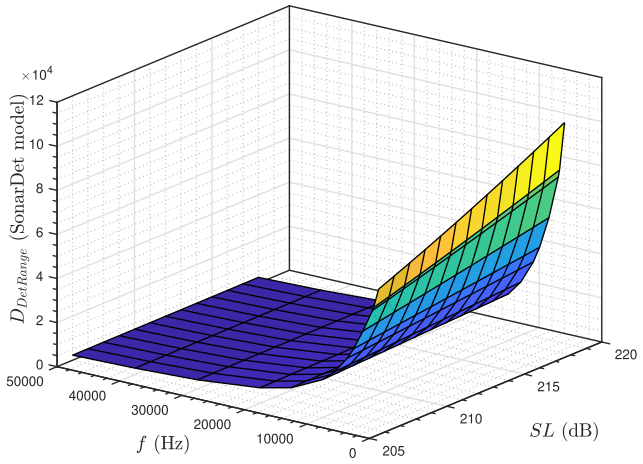

FIGURE 31. Detection Range with respect to *SL* and *f* for $D_{s-r} = 2000$ m (Sonar detection model).

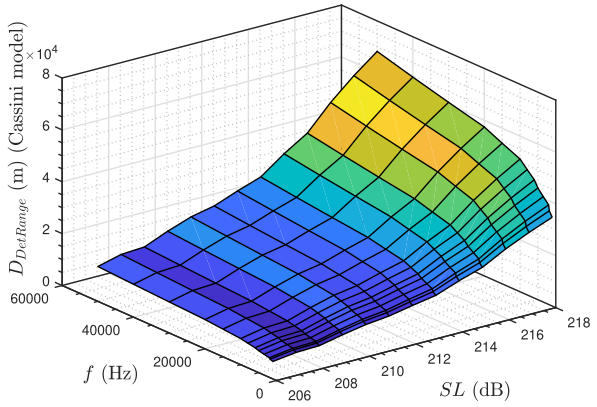

FIGURE 32. Detection Range with respect to *SL* and *f* for $D_{s-r} = 2000$ m (Cassini oval model).

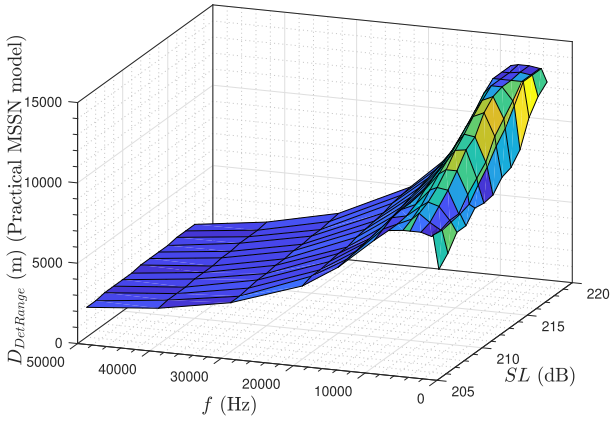

FIGURE 33. Detection Range with respect to *SL* and *f* for $D_{s-r} = 2000$ m (Practical MSSN model).

- When the real target detection distance is found with the practical MSSN model, which considers the environment conditions in practice by using Lybin, the detection range shows a slight increase at low-to-medium frequencies, as shown in Fig. 33. Then it starts to decrease

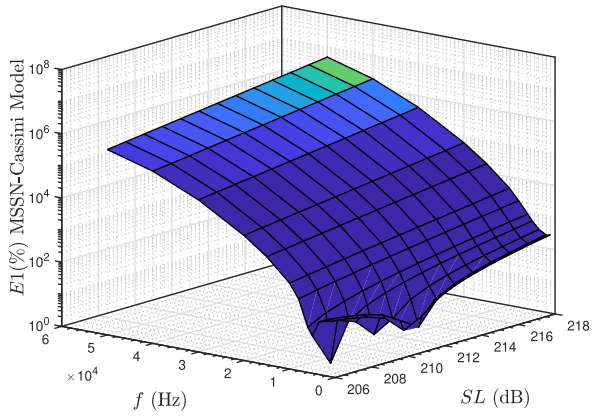

FIGURE 34. The difference between the results yielded by the models, which is a measure of the error in the calculation with respect to *SL* and *f* (Practical MSSN channel model-Cassini oval model).

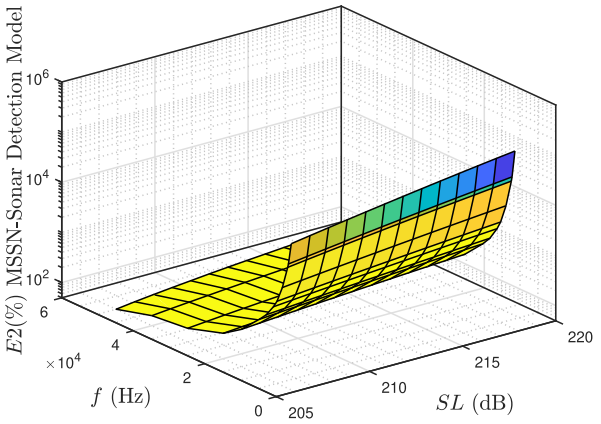

FIGURE 35. The difference between the results yielded by the models, which is a measure of the error in the calculation with respect to *SL* and *f* (Practical MSSN channel model-Sonar detection model).

with frequency. This stems from the idea of designing the ''optimal'' frequency for sonar systems [46], which depends on the spectral variation of the ambient noise and the transmission loss, which is a function of the absorption coefficient [70], [71]. Consequently, the required number of source-receiver pairs first decreases and then increases again in accordance with the detection range.

Therefore, in order to achieve the longest detection range for a sonar system, the optimal frequency relies on the spectral variation of the link budget. In this study, detection range and volume coverage analyses were performed for a windy and noisy environment at sea state 4. Accordingly, in line with our findings, the maximum detection range is obtained at around 3.5 kHz. This is a result of the spectral behavior plotted in Fig. 7 and Fig. 36. For a given source level, the combined effect of the ambient noise and the absorption coefficient leads to the detection ranges in Fig. 33.

Similarly, the curves in Fig.7 given in [72] show how frequency affects the rated source level required to perform detection in a given range. These figures are based on commonly used active sonar equations, detection theory, and noise and attenuation assumptions [73]. For this reason, instead of choosing only the lowest transmission frequency in coverage-guaranteed MSSN deployment placement studies, operational sonar parameters should be determined by frequency-dependent spectral optimization and realistic environmental conditions.

The difference in between the practical MSSN channel model and the Cassini oval model in volume coverage is shown in Fig. 34 as the error rate in relation to frequency and *SL*. When the error rate expression between the models is examined, it is seen that the error level increases as the *SL* increases. However, it is seen that the frequency change in the error rate has a more dominant effect, and the error rate increases dramatically in parallel with the increase in frequency.

The error difference between the MSSN channel model and the sonar detection model is analyzed in Fig. 35. The figure shows that as *SL* increases, there is a slight increase in the error rate between models. However, the actual change occurs with the frequency effect. With the increase in frequency, the error rate between models starts to decrease, unlike the Cassini oval model.

Oceanographic environmental factors such as sound velocity profile, bottom and surface nature are factors that affect the propagation of sound underwater and the performance of sonar systems [74]. Since the performance of sonar systems differs depending on environmental conditions, modeling that considers real environmental conditions is important in terms of real detection range and coverage volume. For this reason, during the creation of the MSSN channel model, the acoustic ray tracing-based Lybin sonar performance prediction tool is used. The spreading factor is obtained depending on the real environment conditions and the practical MSSN channel model is evaluated with the help of Lybin.

When all the above information is examined, it is seen that as mentioned in previous sections, the Cassini oval model, the mostly used method on MSSN coverage, neglects the frequency dependency of the absorption coefficient and only spherical spreading is assumed. Hence, the Cassini oval model gives increasingly erroneous results as the acoustic transmission frequency rises since the spectral variations of $\alpha(f)$ and $NL(f)$ given in Fig. 36 are neglected. Since frequency has a nonlinear effect on the *TL* and *NL* in the sonar equation, it causes different detection ranges and different volume coverage performances depending on the ambient conditions. Therefore, using the Cassini oval model, neglecting the frequency effect, leads to serious errors in MSSN deployment.

On the other hand, in the traditional sonar detection model, which is another model used in MSSN coverage studies, accepting the *m* spreading factor parameter as a constant practical value results in substantial mistakes when computing

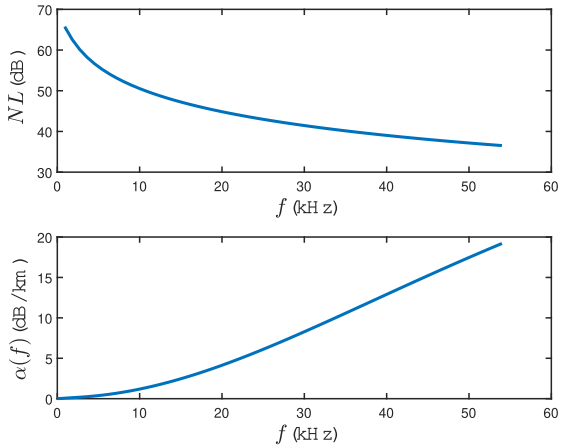

FIGURE 36. Change of NL and α dependent on frequency.

the number of source-receiver pairs and the real detection range. The spreading factor m in the propagation of is significantly impacted by environmental factors such as sound speed profile and variations in the ocean's surface and bottom. Therefore, using the traditional sonar detection model causes major mistakes while deploying MSSN like as Cassini oval model.

Finally, when the error rates depending on the distance between the source-receiver are evaluated, it is as seen Fig. 27 that the error rate between the MSSN and other models increases as the distance between the source receiver increases. As mentioned in Section IV, elliptical, non-convex, and Bernoulli Lemniscate shapes appear in coverage volumes depending on distances and source levels. The main reason for the emergence of these figures is the equivalent detection range value and the active sonar restriction function parameters are essential in obtaining this value.

VIII. CONCLUSION AND FUTURE WORK

In this paper, three-dimensional volume coverage in MSSN is investigated. Previously, coverage in MSSN was studied using Cassini ovals and the traditional sonar detection model in two dimensions, without any discussion on the practicability and feasibility in terms of conditions related to the underwater acoustic propagation environment. In this study, a practical MSSN channel model is proposed, which includes underwater acoustic propagation parameters such as spectral variation of the absorption loss, ambient noise, sound speed profile, and impact of shadow zones. The effect of sound propagation and the ambient conditions is corrected by using Lybin, well-known sonar performance prediction tool, and the model is evaluated. Using practical MSSN channel model, we analyze the coverage problem in a three-dimensional MSSN volume according to the acoustic transmission frequency, distance between the source and the receiver, and source level. Our analysis yields the number of source-receiver pairs to be used to cover a given MSSN volume for various model parameter settings. We compare our results against the Cassini oval and sonar detection models through a volume error expression. The results reveal that the inclusion of ambient conditions, sound propagation characteristics, and frequency-dependent parameters in the acoustic channel model leads to huge error levels in the Cassini oval and traditional sonar detection model, limiting the applicability of these models in realistic MSSN deployment scenarios.

As future work, we are planning to conduct at-sea experiments to measure the coverage efficiency of the source and receiver pairs in accordance with our model using practical mission-critical deployment scenarios. Moreover, our practical MSSN channel model can be extended to include multiple sources and receivers simultaneously. The optimal placement of multiple receivers and sources can be studied in terms of volume coverage and cost.

In addition, different algorithms for the placement of sources and receivers to assure volume coverage in MSSN can be developed. The efficiency of these algorithms requires investigation in terms of performance and computation time.

Finally, signal optimization needs to be developed for the maximization of the detection range in different MSSN sensor placement scenarios.

REFERENCES

[1] R. Lilley, "Recapture wide-area anti-submarine warfare," *Proc. Mag.*, vol. 140, no. 6, p. 1336, 2014.
[2] R. Song, H. Esmaiel, H. Sun, J. Qi, H. Zhang, and M. Zhou, "Multi-submarines detection using multistatic sonar system," in *Proc. IEEE 5th Inf. Technol. Mechatronics Eng. Conf. (ITOEC)*, Jun. 2020, pp. 1671–1675.
[3] E. Miguelanez, P. Patron, K. E. Brown, Y. R. Petillot, and D. M. Lane, "Semantic knowledge-based framework to improve the situation awareness of autonomous underwater vehicles," *IEEE Trans. Knowl. Data Eng.*, vol. 23, no. 5, pp. 759–773, May 2011.
[4] I. F. Akyildiz, D. Pompili, and T. Melodia, "Underwater acoustic sensor networks: Research challenges," *Ad Hoc Netw.*, vol. 3, no. 3, pp. 257–279, Mar. 2005.
[5] B. H. Maranda, "Passive sonar," in *Handbook of Signal Processing in Acoustics*. New York, NY, USA: Springer, 2008, pp. 1757–1781.
[6] S. Kim, B. Ku, W. Hong, and H. Ko, "Performance comparison of target localization for active sonar systems," *IEEE Trans. Aerosp. Electron. Syst.*, vol. 44, no. 4, pp. 1371–1380, Oct. 2008.
[7] Y. Wu, Y. Deng, L. Zhang, Q. Zhang, and R. Bao, "Research on the development of unmanned underwater system detection technology," *J. Phys., Conf.*, vol. 2218, no. 1, Mar. 2022, Art. no. 012079.
[8] R. P. Hodges, *Underwater Acoustics: Analysis, Design and Performance of Sonar*. Hoboken, NJ, USA: Wiley, 2011.
[9] A. C. Coon, "Spatial correlation of detections for impulsive echo ranging sonar," *Johns Hopkins APL Tech. Dig.*, vol. 18, no. 1, pp. 105–112, 1997.
[10] T. Jia, X. Shen, and H. Wang, "Multistatic sonar localization with a transmitter," *IEEE Access*, vol. 7, pp. 111192–111203, 2019.
[11] D. Orlando, F. Ehlers, and N. Kolev, "Advances in multistatic sonar," in *Sonar Systems*. Rijeka, Croatia: Intech, 2011, pp. 29–50.
[12] E. Özer and A. K. Hocaoğlu, "Robust model-dependent Poisson multi Bernoulli mixture trackers for multistatic sonar networks," *IEEE Access*, vol. 9, pp. 163612–163624, 2021.
[13] O. Erdinc, P. Willett, and S. Coraluppi, "Multistatic sensor placement: A tracking approach," in *Proc. 9th Int. Conf. Inf. Fusion*, Jul. 2006, pp. 1–8.
[14] D. Grimmett and S. Coraluppi, "Contact-level multistatic sonar data simulator for tracker performance assessment," in *Proc. 9th Int. Conf. Inf. Fusion*, Jul. 2006, pp. 1–7.
[15] A. Saffari, Seyed-hamid Zahiri, and M. Khishe, "Automatic recognition of sonar targets using feature selection in micro-Doppler signature," *Defence Technol.*, 2022.
[16] M. Khishe and A. Safari, "Classification of sonar targets using an MLP neural network trained by dragonfly algorithm," *Wireless Pers. Commun.*, vol. 108, no. 4, pp. 2241–2260, Oct. 2019.

[17] D. Pompili, T. Melodia, and I. F. Akyildiz, "Deployment analysis in underwater acoustic wireless sensor networks," in *Proc. 1st ACM Int. Workshop Underwater Netw. (WUWNet)*, 2006, pp. 48–55.

[18] M. Karatas, E. Craparo, and A. Washburn, "A cost effectiveness analysis of randomly placed multistatic sonobuoy fields," in *Proc. Int. Workshop Appl. Model. Simul. (WAMS)*, 2014. [Online]. Available: https://www.researchgate.net/publication/305721029_A_COST_EFFECTIVENESS_ANALYSIS_OF_RANDOMLY_PLACED_MULTISTATIC_SONOBUOY_FIELDS

[19] J. Lu, X. Sheng, Q. Ling, J. Xu, and Y. Yuan, "The research on the coverage area of multistatic sonar under various work modes," in *Proc. OCEANS*, San Diego, CA, USA, Sep. 2013, pp. 1–4.

[20] A. R. Washburn, "A multistatic sonobuoy theory," Naval Postgraduate School Monterey CA, Tech. Rep., 2010.

[21] A. Washburn and M. Karataş, "Multistatic search theory," *Mil. Oper. Res.*, vol. 20, no. 1, pp. 21–38, 2015.

[22] M. Karatas and G. Akman, *GelisigüZel Olusturulmus Multistatik SensöR Sahalarinin Performans Tahmini*, vol. 16, no. 47. İzmir, Turkey: Dokuz Eylül Üniversitesi Mühendislik Fakültesi Fen ve Mühendislik Dergisi, May 2014.

[23] D. R. DelBalzo, D. N. McNeal, and D. P. Kierstead, "Optimized multistage sonobuoy fields," in *Proc. Eur. Oceans*, vol. 2, Jun. 2005, pp. 1193–1198.

[24] D. R. DelBalzo and K. C. Stangl, "Design and performance of irregular sonobuoy patterns in complicated environments," in *Proc. OCEANS*, Oct. 2009, pp. 1–4.

[25] J. M. Hovem, "Ray trace modeling of underwater sound propagation," in *Modeling and Measurement Methods for Acoustic Waves and for Acoustic Microdevices*. London, U.K.: IntechOpen, 2013.

[26] K. E. Andreassen and K. T. Hjelmervik, "Modelled sonar and target depth distributions for active sonar operations in realistic environments," in *Proc. Meetings Acoust.*, vol. 47, no. 1. USA: Acoustical Society of America, 2022, Art. no. 070013.

[27] M. A. Ainslie, *Principles of Sonar Performance Modelling*, vol. 707. Berlin, Germany: Springer, 2010.

[28] R. van Vossen, E. J. Eidem, S. Ivansson, B. Chalindar, J. Dybedal, M. E. Colin, F. P. Benders, B. L. Andersson, B. Juhel, X. Cristol, and G. K. Olsen, "Improved active sonar tactical support by through-the-sensor estimation of acoustic seabed properties," *IEEE J. Ocean. Eng.*, vol. 39, no. 4, pp. 755–768, Oct. 2014.

[29] *LYBIN 6.0—User Manual*. [Online]. Available: https://publications.ffi.no/nb/item/asset/dspace:3714/11-00205.pdf

[30] P. Sun and A. Boukerche, "Modeling and analysis of coverage degree and target detection for autonomous underwater vehicle-based system," *IEEE Trans. Veh. Technol.*, vol. 67, no. 10, pp. 9959–9971, Oct. 2018.

[31] M. Cardei and J. Wu, "Coverage in wireless sensor networks," in *Handbook of Sensor Networks*, vol 21. USA: CRC Press, 2004, pp. 201–202.

[32] P. N. Ngatchou, W. L. J. Fox, and M. A. El-Sharkawi, "Multiobjective multistatic sonar sensor placement," in *Proc. IEEE Int. Conf. Evol. Comput.*, Jul. 2006, pp. 2713–2719.

[33] M. Fewell and S. Ozols, "Simple detection-performance analysis of multistatic sonar for anti-submarine warfare," DSTO Defence Sci. Technol., Canberra, Australia, Tech. Rep. DSTO-TR-2562, 2011.

[34] M. Karatas, E. Craparo, and G. Akman, "Bistatic sonobuoy deployment strategies for detecting stationary and mobile underwater targets," *Nav. Res. Logistics*, vol. 65, no. 4, pp. 331–346, Jun. 2018.

[35] M. Karatas and B. Gundogdu, "Using simulation for locating transmitter in a multistatic sensor network," in *Proc. 9th Int. Conf. Recent Adv. Space Technol. (RAST)*, Jun. 2019, pp. 521–526.

[36] A. Fügenschuh, and E. M. Craparo, *The Multistatic Sonar Location Problem Mixed-Integer Program.* Germany: Springer, 2017.

[37] T. U. Kuhn, "Optimal sensor placement in active multistatic sonar networks," Ph.D. dissertation, Naval Postgraduate School, Monterey, CA, USA, 2014.

[38] C. Hof, "Optimization of source and receiver placement in multistatic sonar environments," Ph.D. dissertation, Naval Postgraduate School, Monterey, CA, USA, 2015.

[39] E. M. Craparo, M. Karatas, and T. U. Kuhn, "Sensor placement in active multistatic sonar networks," *Nav. Res. Logistics*, vol. 64, no. 4, pp. 287–304, Jun. 2017.

[40] E. M. Craparo and M. Karatas, "A method for placing sources in multistatic sonar networks," Naval Postgraduate School, Monterey, CA, USA, Tech. Rep. NPS-OR-18-001, 2018.

[41] E. Craparo and M. Karatas, "Optimal source placement for point coverage in active multistatic sonar networks," *Nav. Res. Logistics*, vol. 67, no. 1, pp. 63–74, Feb. 2020.

[42] E. M. Craparo, A. Fügenschuh, C. Hof, and M. Karatas, "Optimizing source and receiver placement in multistatic sonar networks to monitor fixed targets," *Eur. J. Oper. Res.*, vol. 272, no. 3, pp. 816–831, Feb. 2019.

[43] M. Karatas, "Optimal deployment of heterogeneous sensor networks for a hybrid point and barrier coverage application," *Comput. Netw.*, vol. 132, pp. 129–144, Feb. 2018.

[44] E. Yakıcı and M. Karatas, "Solving a multi-objective heterogeneous sensor network location problem with genetic algorithm," *Comput. Netw.*, vol. 192, Jun. 2021, Art. no. 108041.

[45] M. Karatas, "A multi-objective bi-level location problem for heterogeneous sensor networks with hub-spoke topology," *Comput. Netw.*, vol. 181, Nov. 2020, Art. no. 107551.

[46] R. J. Urick, *Principles of Underwater Sound-2*. New York, NY, USA: McGraw-Hill, 1975.

[47] J. I. Bowen and R. W. Mitnick, "A multistatic performance prediction methodology," in *Johns Hopkins APL Tech. Dig.*, vol. 20, no. 3, 1999, p. 425.

[48] C. H. Sherman and J. L. Butler, "Electroacoustic transduction," in *Transducers and Arrays for Underwater Sound*. New York, NY, USA: Springer, 2007, pp. 31–75.

[49] A. D. Waite, *Sonar for Practising Engineers*. Hoboken, NJ, USA: Wiley, 2002.

[50] L. Bjørnø, "Scattering of sound," in *Applied Underwater Acoustics*. Amsterdam, The Netherlands: Elsevier, 2017, pp. 297–362.

[51] M. A. Çavuşlu, M. A. Altuncu, H. Özcan, F. K. Gülağz, and S. Şahin, "Estimation of underwater acoustic channel parameters for Erdek/Turkey region," *Appl. Acoust.*, vol. 181, Oct. 2021, Art. no. 108135.

[52] M. Stojanovic, "On the relationship between capacity and distance in an underwater acoustic communication channel," *ACM SIGMOBILE Mobile Comput. Commun. Rev.*, vol. 11, no. 4, pp. 34–43, 2007.

[53] M. Ainslie, P. Dahl, and C. De Jong, "Practical spreading laws: The snakes and ladders of shallow water acoustics," in *Proc. 2nd Int. Conf. Exhib. Underwater Acoust.*, 2014, pp. 22–27.

[54] W. A. Kuperman and P. Roux, "Underwater acoustics," in *Handbook of Acoustics*, T. D. Rossing, Ed. New York, NY, USA: Springer, 2014.

[55] M. Karataş, "A multi foci closed curve: Cassini oval, its properties and applications," Doğuş Üniversitesi Dergisi, vol. 2, no. 14, pp. 231–248, Jul. 2013.

[56] P. Grabusts, "Different approaches to clustering—Cassini ovals," *Inf. Technol. Manage. Sci.*, vol. 20, no. 1, pp. 30–33, Jan. 2017.

[57] H. Cox, "Fundamentals of bistatic active sonar," in *Underwater Acoustic Data Processing*, Y. Chan, Ed. Dordrecht, The Netherlands: Springer, 1989, pp. 3–24.

[58] M. Karataş and G. Akman, "Bistatic sonobuoy deployment configuration for stationary targets," *J. Nav. Sci. Eng.*, vol. 11, no. 2, pp. 1–10, 2015.

[59] E. Cayirci, H. Tezcan, Y. Dogan, and V. Coskun, "Wireless sensor networks for underwater survelliance systems," *Ad Hoc Netw.*, vol. 4, no. 4, pp. 431–446, Jul. 2006.

[60] E. Dombestein, S. Mjølsnes and F. Hermansen, "Visualization of sonar performance within environmental information," in *Proc. MTS/IEEE OCEANS*, Bergen, Norway, 2013, pp. 1–6, doi: 10.1109/OCEANS Bergen.2013.6608090.

[61] C. Bassett, J. Thomson, P. H. Dahl, and B. Polagye, "Flow-noise and turbulence in two tidal channels," *J. Acoust. Soc. Amer.*, vol. 135, no. 4, pp. 1764–1774, Apr. 2014.

[62] R. Revathy and P. R. S. Pillai, "Effect of wind speed in undersea acoustic communications," in *Proc. OCEANS* Chennai, Feb. 2022, pp. 1–4.

[63] P. H. Dahl, J. H. Miller, D. H. Cato, and R. K. Andrew, "Underwater ambient noise," *Acoust. Today*, vol. 3, no. 1, pp. 23–33, 2007.

[64] A. Bereketli, "Remotely powered underwater acoustic sensor networks," Ph.D. dissertation, Dept. Elect. Electron. Eng., Middle East Tech. Univ., Ankara, Turkey, 2013. [Online]. Available: http://etd.lib.metu.edu.tr/upload/12615958/index.pdf

[65] K. T. Hjelmervik and E. M. Bøhler, "Optimization of active sonar parameters in a measured environment," in *Proc. Meetings Acoust.* USA: Acoustical Society of America, 2021, Art. no. 070006.

[66] Z. Ziling, F. Erzheng, Y. Xuanzi, and G. Chenyang, "Detection performance analysis of multistatic sonar system based on cumulative detection," in *Proc. OES China Ocean Acoust. (COA)*, 2021, pp. 601–608.

[67] S. Xie. (Jan. 2019). *Disc Method*. [Online]. Available: https://medium.com/self-study-calculus/disc-method-38d9380b57c1

[68] G. B. Thomas, M. D. Weir, J. Hass, and F. R. Giordano, *Thomas' Calculus*. Reading, MA, USA: Addison-Wesley, 2005.
[69] (2021). *AN/SSQ-565 Multistatic Low Frequency Active Source Sonobuoy*. [Online]. Available: https://www.ultra.group/media/2663/anssq-565-datasheet_final.pdf
[70] J. Stewart, E. Westerfield, and M. Brandon, "Optimum frequencies for active sonar," *J. Acoust. Soc. Amer.*, vol. 32, no. 7, p. 927, 1960.
[71] J. L. Stewart, E. C. Westerfield, and M. K. Brandon, "Optimum frequencies for noise-limited active sonar detection," *J. Acoust. Soc. Amer.*, vol. 70, no. 5, pp. 1336–1338, Nov. 1981.
[72] G. D. Tyler, "The emergence of low-frequency active acoustics as a critical antisubmarine warfare technology," *Johns Hopkins APL Tech. Dig.*, vol. 13, no. 1, 1992, pp. 145–159.
[73] E. McCutcheon, M. T. Haggett, and A. E. UK, "Counting the ASW calories: Maximising sonar performance under weight and size constraints," in *Proc. UDT*, Stockholm, Sweden, 2019. [Online]. Available: https://www.udt-global.com/_media/libraries/platform-design/102—Ewan-McCutcheon-Paper.pdf
[74] H. O. Sertlek, M. A. Ainslie, and K. D. Heaney, "Analytical and numerical propagation loss predictions for gradually range-dependent isospeed waveguides," *IEEE J. Ocean. Eng.*, vol. 44, no. 4, pp. 1240–1252, Oct. 2019.

ALPER AVCIOGLU (Graduate Student Member, IEEE) received the B.Sc. degree from the Department of Control Engineering, Istanbul Technical University, Istanbul, Turkey, in 2011, and the M.Sc. degree in electrical and electronics engineering from Hacettepe University, Ankara, Turkey, in 2015. He is currently pursuing the Ph.D. degree in information systems with the Information Institute, Gazi University, Ankara. Since 2011, he has been working as an Underwater Acoustic Systems Engineer at the Defence Systems Technologies Division, Aselsan Inc. His research interests include underwater acoustic systems, hull-mounted sonars, multistatic sonars, and underwater sonar sensor networks.

ALPER BEREKETLI (Member, IEEE) was born in Izmir, Turkey, in 1980. He received the B.S., M.S., and Ph.D. degrees in electrical and electronics engineering from Middle East Technical University, Ankara, Turkey, in 2002, 2005, and 2013, respectively. From 2002 to 2009, he was a Research and Teaching Assistant at the Department of Electrical and Electronics Engineering, Middle East Technical University. He worked as a Chief Systems Engineer at Meteksan Savunma, Ankara, from 2009 to 2016. Since 2016, he has been with Aselsan Inc., Ankara. He is currently a Senior Lead Waveform Design Engineer at the Communication and Information Technologies Division. His research interests include next-generation wireless communications and sensor networks, and their applications to flying ad hoc networks, energy harvesting wireless communications, and underwater acoustic systems.

OMER FARUK BAY received the B.Sc. degree in electrical and electronics education from Gazi University, Turkey, in 1985, and the M.Sc. and Ph.D. degrees in electronics engineering from Erciyes University, Turkey, in 1992 and 1996, respectively. He is currently a Full Professor at the Department of Electrical and Electronics Engineering, Gazi University. His research interests include artificial intelligence and its applications, control and instrumentation, intelligent systems, and BCI for home automation.